

Supporting Information

Reversible Conformational Switching of a Photo-
Responsive *ortho*-azobenzene/2,6-
pyridyldicarboxamide Foldamer

Sarah J. Pike,^{a,b*} Richard Telford^b and Louise Male,^a

^aSchool of Chemistry, University of Birmingham, Edgbaston, Birmingham, B15 2TT, UK.

^bFaculty of Life Sciences, University of Bradford, Bradford, West Yorkshire, BD7 1DP, UK

Email: s.j.pike@bham.ac.uk

Contents	<i>S2</i>
General Experimental Details	<i>S3</i>
Crystallographic Details	<i>S5</i>
Synthetic Details	<i>S7</i>
COSY and NOESY Studies	<i>S11</i>
Photoswitching Studies: UV/Vis Spectroscopy	<i>S13</i>
Photoswitching Studies: CD Spectroscopy	<i>S16</i>
Photoswitching Studies: ¹H NMR Spectroscopy	<i>S20</i>
Crystal Data and Structural Refinement	<i>S31</i>
Solid-State Analysis	<i>S33</i>
Appendix: ¹H and ¹³C NMR spectra	<i>S46</i>
References	<i>S52</i>

General Experimental Details

All NMR spectroscopy was carried out on a Bruker AVIII300, Bruker AVIII400, Bruker NEO400 and Bruker AV4-500 NMR spectrometer using the residual solvent as the internal standard. All the chemical shifts (δ) are quoted in ppm and coupling constants are given in Hz and are rounded to 0.1 Hz. Splitting patterns are abbreviated as follows: s (singlet), br (broad), d (doublet), t (triplet), m (multiplet) or some combination of these. Thin layer chromatography (TLC) was performed using commercially available precoated (Macherey-Nagel alugram. Sil G/UV254) and visualized with UV light at 254 nm. Flash column chromatography was carried out using Fluorochem Davisil 40-63u 60Å. Melting points were obtained on a Gallenkemp melting point apparatus and are uncorrected. Mass spectra were obtained using Waters LCT (ES), Waters Synapt (ES) or Bruker MicroTOF spectrometers, each fitted with TOF detector. UV/Vis spectroscopy was carried out on an Agilent Cary 3500 UV/Vis photospectrometer with a variable temperature control unit. All UV/Vis spectra were run at 298 K. The thermal *cis-trans* isomerisation process of **1** was monitored, under non-irradiative conditions, at 298 K using an Agilent Cary 3500 UV/Vis photospectrometer fitted with a variable temperature control unit. Infrared spectroscopy was carried out on a PerkinElmer Spectrum Two FT-IR spectrometer. Circular dichroism (CD) spectroscopy was carried out on a Jasco J-715 Spectropolarimeter. The optical chamber was purged with nitrogen and kept under a nitrogen atmosphere throughout the duration of the experiments. Petrol refers to the fraction of light petroleum ether boiling between 40 and 60 °C. Chloroform and acetone were purchased from Fisher chemicals. Ethyl acetate, petrol and methanol were purchased from VWR. Dichloromethane, 2'-aminoacetanilide and potassium hydroxide were purchased from Sigma Aldrich. Pyridine, 2,6-dicarbonylchloride and 4 Å molecular sieves were purchased from Acros Organic. Pyridine was purchased from Fluorochem. All chemicals were used as received. **3** and **4** were prepared using known literature procedures.^{1,2} Single crystals of **4** suitable for X-

ray diffraction analysis were obtained by slow diffusion of di-isopropyl ether into a saturated solution of the compound in chloroform.

The following abbreviations are employed: Ac = acetyl, aq. = aqueous, Ar = aromatic, br = broad, calcd. = calculated, circular dichroism = CD, d = doublet, eq. = equivalent(s), Et = ethyl, g = gram(s), h = hour(s), Hz = Hertz, IR = infrared, m = multiplet, Me = methyl, min = minute(s), m.p. = melting point, pet. = petroleum, Ph = phenyl, PSS = photostationary state, q = quartet, s = singlet and t = triplet.

Crystallographic Details

The dataset for **1** was measured by the UK National Crystallography Service on a Rigaku 007HF diffractometer equipped with HF Varimax confocal mirrors, a AFC11 goniometer and HyPix 6000HE detector. A suitable single crystal of **4** was selected and the data was collected on a SuperNova, Dual, Cu at home/near, Atlas diffractometer. The data collection was driven and processed and an absorption correction was applied using CrysAlisPro.⁶ These structures were solved using ShelXT⁴ and were refined by a full-matrix least-squares procedure on F² in ShelXL.⁵ Figures and reports were produced using OLEX2.³ All non-hydrogen atoms were refined with anisotropic displacement parameters. The CCDC number for **1** is 2121319 and for **4** is 2130347.

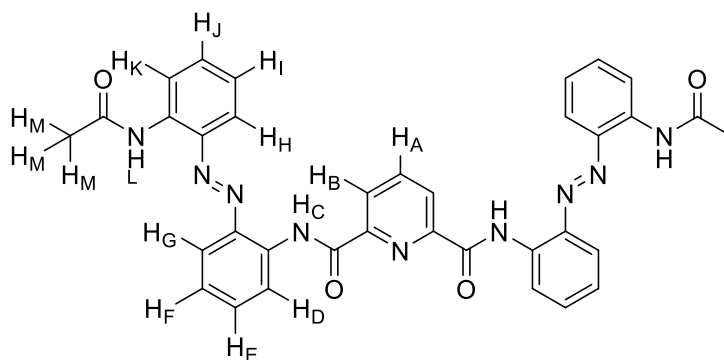
Details for 1: The crystal was a two-component non-merohedral twin with the domains being related by -178.95° about the reciprocal direction $[0.89\ 0.00\ 0.45]$. The refined percentage ratio of the domains is 44.76 (11) : 55.24 (11). The structure occupies a non-centrosymmetric space group, $P\ 1$, and the Flack parameter has been refined as 0.019 (11). The structure is thus shown to be a single enantiomer with C(20), C(47), C(120) and C(147) all being S in every case. The structure contains two crystallographically-independent molecules and three molecules of chloroform, two of which are disordered over two positions each. In the case of C(301), Cl(31), Cl(32), Cl(33) and C(31A), Cl(1A), Cl(2A), Cl(3A) the refined percentage occupancy ratio of the two positions is 63.3 (8) : 36.7 (8). In the case of C(401), Cl(41), Cl(42), Cl(43) and C(41B),

Cl(1B), Cl(2B), Cl(3B) the refined percentage occupancy ratio of the two positions is 51.3 (6) : 48.7 (6). The disordered molecules were refined subject to restraints on geometry and thermal parameters. The hydrogen atoms bonded to N(2), N(5), N(6), N(9), N(102), N(105), N(106) and N(109) were located in the electron density and their positions refined subject to bond distance restraints (in all cases apart from that bonded to N(105) for which the position was refined freely). All remaining hydrogen atoms were fixed as riding models and, for all hydrogen atoms in the structure the isotropic thermal parameters (U_{iso}) were based on the U_{eq} of the parent atom.

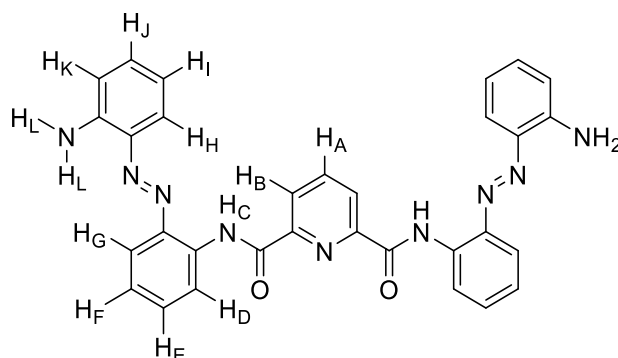
Details for 4: The structure occupies a non-centrosymmetric space group but it has not been possible to determine a reliable Flack parameter and thus the absolute structure is unknown. The hydrogen atoms bonded to N(1) and N(4) were located in the electron density and the positions freely refined. The remaining hydrogen atoms were fixed as riding models and the isotropic thermal parameters (U_{iso}) of all hydrogen atoms were based on the U_{eq} of the parent atom.

Synthetic Details

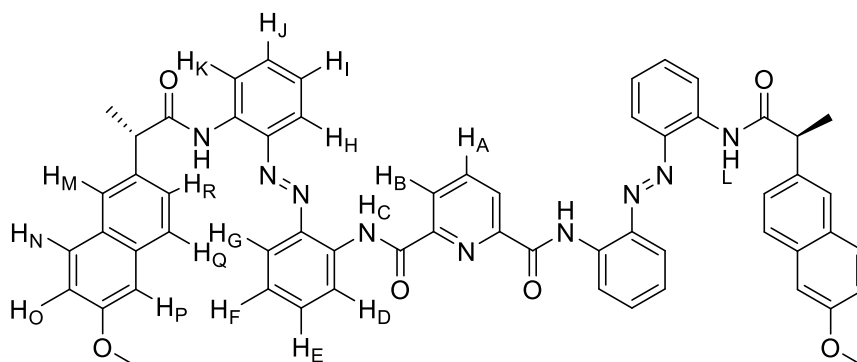
5



To a solution of 2-acetamido-2'-amino-*ortho*-azobenzene (0.25 g, 0.98 mmol) in CH₂Cl₂ (5 mL) was added pyridine (2 mL) and 4 Å molecular sieves (0.30 g) and the resultant bright red solution was left stirring at ambient temperature for 30 min. After this time, pyridine-2,6-dicarbonylchloride (0.09 g, 0.05 mmol) was added to the reaction mixture and the resultant solution was left stirring for 18 h at ambient temperature. The 4 Å molecular sieves were removed by filtration and diluted with CH₂Cl₂ (30 mL), washed with water (50 mL) and brine (50 mL), dried over MgSO₄, filtered off and concentrated under reduced pressure. The resultant residue was subjected to flash column chromatography (CHCl₃/MeOH: 98/2) to yield the desired compound as an orange solid. (0.33 g, 52%). m.p.: 286-287 °C; ¹H NMR (400 MHz, CDCl₃, 298 K): δ 11.56 (2H, br, s, NH_C), 8.94 (2H, dd, ³J = 8.4 Hz, ⁴J = 1.6 Hz, H_H), 8.88 (2H, br, s, NH_L), 8.61 (2H, d, ³J = 8.0 Hz, H_B), 8.43 (2H, dd, ³J = 8.0 Hz, ⁴J = 1.2 Hz, H_G), 8.24 (1H, t, ³J = 7.6 Hz, H_A), 7.59 (2H, td, ³J = 7.2 Hz, ⁴J = 1.6 Hz, H_I), 7.38 (2H, dd, ³J = 8.0 Hz, ⁴J = 1.6 Hz, H_D), 7.29-7.26 (2H, m, H_K), 7.14 (2H, td, ³J = 7.2 Hz, ⁴J = 1.2 Hz, H_J), 6.87 (2H, td, ³J = 7.2 Hz, ⁴J = 1.6 Hz, H_F), 6.19 (2H, td, ³J = 7.2 Hz, ⁴J = 1.2 Hz, H_E), 2.21 (3H, s, 2 × CH₃, H_M); ¹³C NMR (100 MHz, CDCl₃, 298 K): δ 167.0, 161.9, 150.3, 140.4, 140.2, 138.9, 137.9, 137.6, 133.8, 133.5, 126.5, 124.5, 123.4, 120.7, 119.7, 116.3, 115.4, 25.6; IR (solid) ν_{max} 3387, 3350, 3081, 1706, 1697, 1678, 1589, 1504, 1438, 1365, 1286, 1240, 1224, 1152, 1133 cm⁻¹; LR-ESI(+ve) m/z 640; HR-ESI(+ve): calcd. 640.2421 found 640.2438 for C₃₅H₃₀N₉O₄.



To a solution of **1** (0.063 g, 0.098 mmol) in H₂O/MeOH/acetone (3/9/9 mL) was added KOH (0.069 g, 0.13 mmol) and the bright red reaction mixture was heated to 80 °C for 18 h. After this time, the homogeneous bright red solution was allowed to cool to room temperature and the excess solvent was removed under reduced pressure. The resultant residue was extracted with CH₂Cl₂ (3 × 45 mL) and the organic layers were combined, dried over MgSO₄, filtered off and concentrated under reduced pressure. The resultant residue was subjected to flash column chromatography (EtOAc/Pet. Ether: 1/4) to yield the desired compound as a bright red solid (0.025 g, 45%). m.p.: did not decompose or melt up to 300 °C; ¹H NMR (400 MHz, CDCl₃, 298 K): δ 11.7 (2H, br, s, NH_C), 8.79 (2H, dd, ³J = 8.0 Hz, ⁴J = 1.2 Hz, H_H), 8.55 (2H, d, ³J = 7.6 Hz, H_B), 8.20 (1H, t, ³J = 7.6 Hz, H_A), 7.45 (2H, td, ³J = 7.2 Hz, ⁴J = 1.2 Hz, H_I), 7.38 (4H, dd, ³J = 7.6 Hz, ⁴J = 0.8 Hz, H_{D+K}), 7.05 (2H, td, ³J = 7.2 Hz, ⁴J = 1.2 Hz, H_J), 6.67 (2H, td, ³J = 6.8 Hz, ⁴J = 1.2 Hz, H_F), 6.34 (2H, dd, ³J = 8.0 Hz, ⁴J = 1.2 Hz, H_G), 6.06 (2H, td, ³J = 6.8 Hz, ⁴J = 1.6 Hz, H_E), 5.03 (4H, s, br, 2 × NH₂, H_L); ¹³C NMR (100 MHz, CDCl₃, 298 K): δ 161.4, 150.1, 144.7, 140.9, 139.8, 137.8, 135.6, 132.7, 131.4, 125.7, 124.0, 121.1, 120.2, 117.7, 117.3, 116.6; IR (solid) ν_{max} 3322, 1671, 1614, 1588, 1513, 1482, 1447, 1314, 1207, 1068 cm⁻¹; LR-ESIMS (+ve): 279 [M+2H]²⁺; 556 [M+H]⁺; HRESI(+ve): calcd. 556.2204 found 556.2187 for C₃₁H₂₆O₂N₉.



To a solution of **6** (0.12 g, 0.22 mmol) in CH₂Cl₂ (2 mL) was added pyridine (0.50 mL) and the resultant red solution was stirred at ambient temperature for 30 min. After this time, (*S*)-(+)-naproxen chloride (0.33 g, 1.3 mmol) was added to the reaction mixture and the resultant bright orange solution was stirred at ambient temperature for 48 h. Whereupon, the reaction mixture was diluted with CH₂Cl₂ (10 mL) and washed with H₂O (3 × 5 mL) and brine (5 mL), the organic layer was dried over MgSO₄, filtered off and concentrated under reduced pressure. The resultant residue was subjected to flash column chromatography (EtOAc/Pet. Ether: 60/40) to yield the desired product as an orange solid (0.16 g, 72%). Single crystals suitable for X-ray diffraction analysis were obtained by slow diffusion of di-isopropyl ether into a saturated solution of the compound in chloroform. ¹H NMR (400 MHz, CDCl₃, 298 K): δ 11.23 (2H, s, br, NH_C), 8.86 (2H, s, NH_L), 8.78 (2H, dd, ³J = 8.0 Hz, ⁴J = 1.2 Hz, H_H), 8.69 (2H, dd, ³J = 8.0 Hz, ⁴J = 1.2 Hz, H_G), 8.53 (2H, d, ³J = 8.0 Hz, H_B), 8.16 (1H, t, ³J = 7.8 Hz, H_A), 7.84-7.75 (6H, m, H_{M+P+Q}), 7.41 (2H, dd, ³J = 7.8 Hz, ⁴J = 1.2 Hz, H_R), 7.35 (2H, td, ³J = 7.2 Hz, ⁴J = 1.0 Hz, H_I), 7.27-7.24 (2H, m, H_N), 7.19-7.14 (4H, m, H_{D+O}), 6.78 (2H, td, ³J = 7.6 Hz, ⁴J = 1.2 Hz, H_F), 6.15 (2H, td, ³J = 8.0 Hz, ⁴J = 1.6 Hz, H_J), 5.94 (2H, td, ³J = 7.6 Hz, ⁴J = 1.2 Hz, H_E), 5.81 (2H, dd, ³J = 8.0 Hz, ⁴J = 1.6 Hz, H_K), 4.11 (2H, q, 6.78 ³J = 7.2 Hz, CH), 3.96 (6H, s, OCH₃), 1.73 (6H, d, ³J = 7.2 Hz, CH₃); ¹³C NMR (100 MHz, CDCl₃, 298 K): δ 173.0, 161.5, 158.2, 149.9, 139.75, 139.71, 138.7, 137.9, 137.1, 136.3, 134.1, 132.96, 132.95, 129.6, 129.4,

128.2, 127.8, 126.5, 126.1, 123.8, 122.9, 120.0, 119.6, 119.1, 114.9, 114.0, 106.1, 55.6, 48.5, 19.1; UV/Vis: $\lambda_{\text{max}}(\text{MeCN})/\text{nm}$ 306 ($\epsilon/\text{dm}^3 \text{ mol}^{-1} \text{ cm}^{-1}$ 28 200), 332 (21 600), 412 (13 000) and 464 (6 900); (LR-ESIMS (+ve): 980 $[\text{M}+\text{H}]^+$; HRESI(+ve): calcd. 980.3879 found 980.3878 for $\text{C}_{59}\text{H}_{50}\text{O}_6\text{N}_9$.

COSY and NOESY spectra of 1

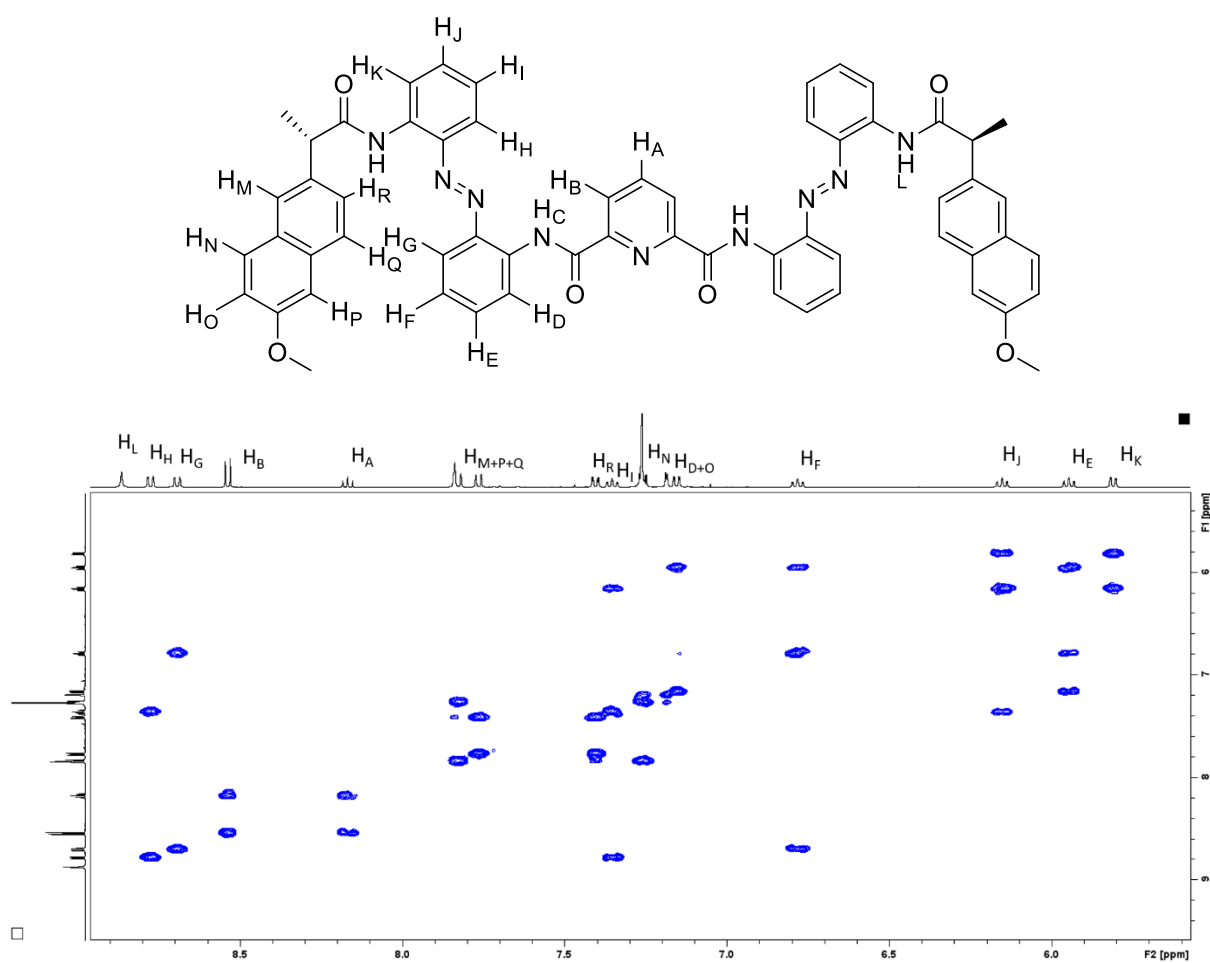


Figure S1. Partial COSY NMR spectrum of **1** (400 MHz, CDCl₃, 298 K)

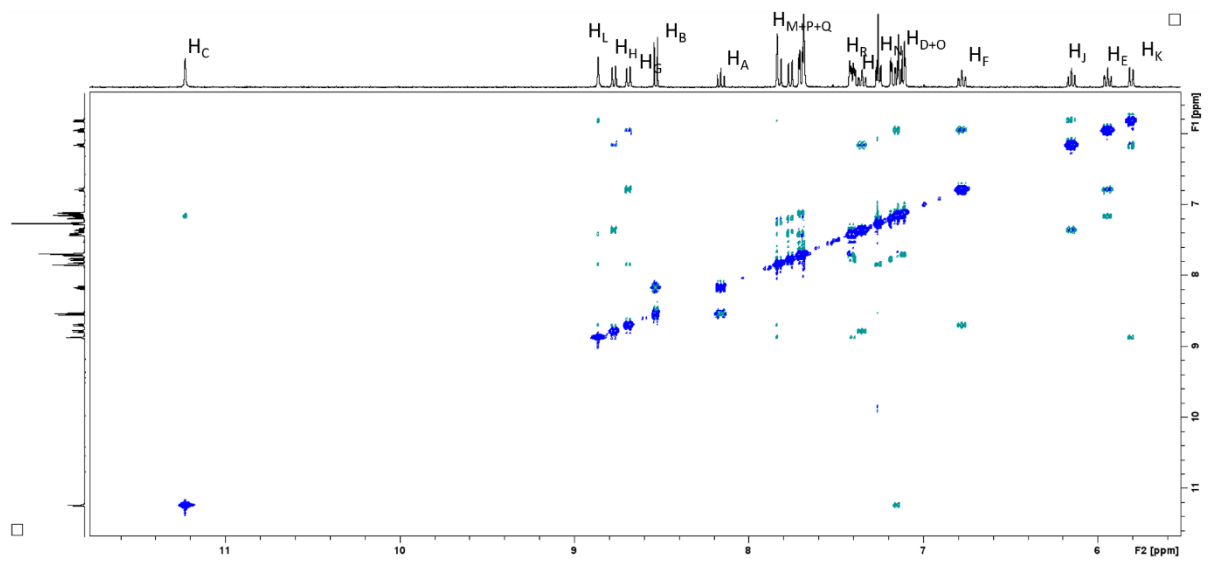


Figure S2. Partial NOESY NMR spectrum of **1** (400 MHz, CDCl₃, 298 K)

Photoswitching Studies: UV/Vis Spectroscopy

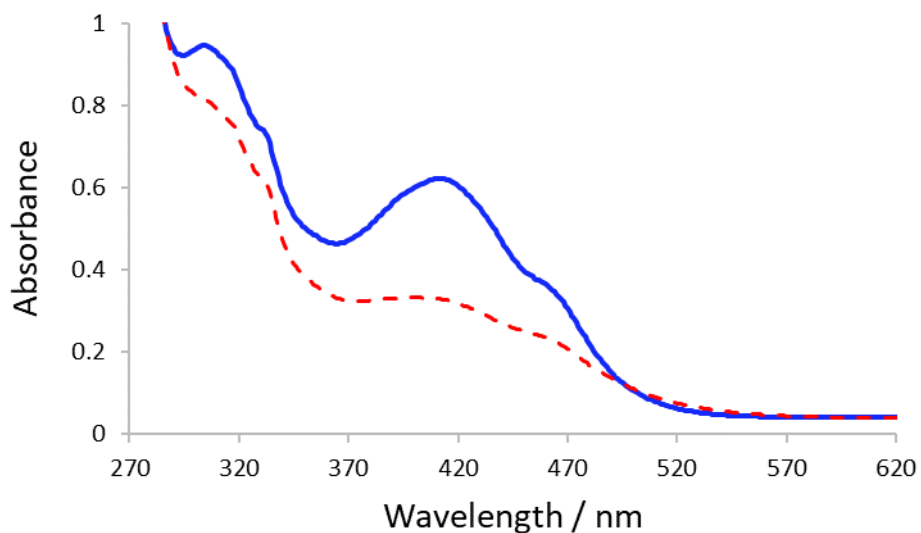


Figure S3. UV/Vis spectra of **1** before irradiation (shown in blue line) and at the photostationary state (PSS) (shown in the dashed red line) after irradiation at 365 nm for 10 min.

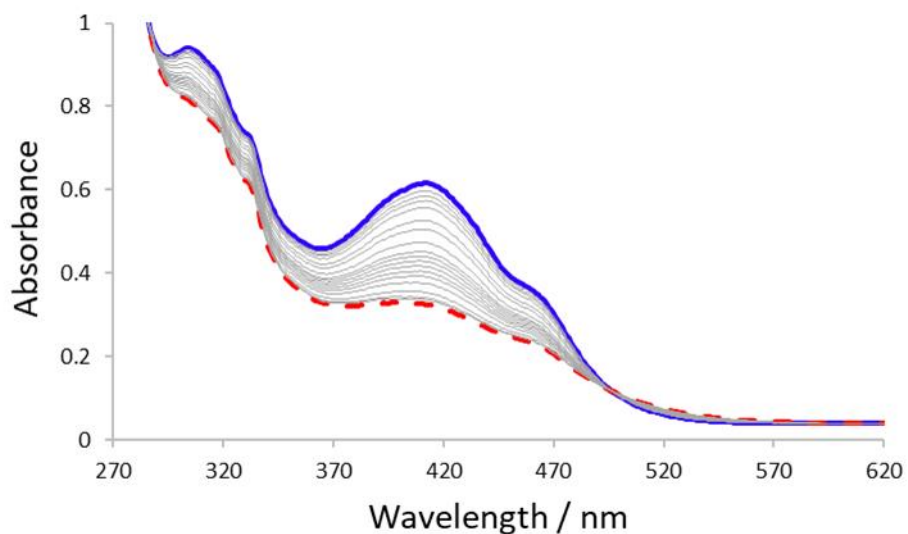


Figure S4. UV/Vis spectra of **1** before irradiation (shown in blue line) and at the photostationary state (PSS) (shown in the dashed red line) after irradiation at 365 nm for 10 min. Grey lines show the thermal relaxation of **1** observed after irradiation at 365 nm for 10 min.

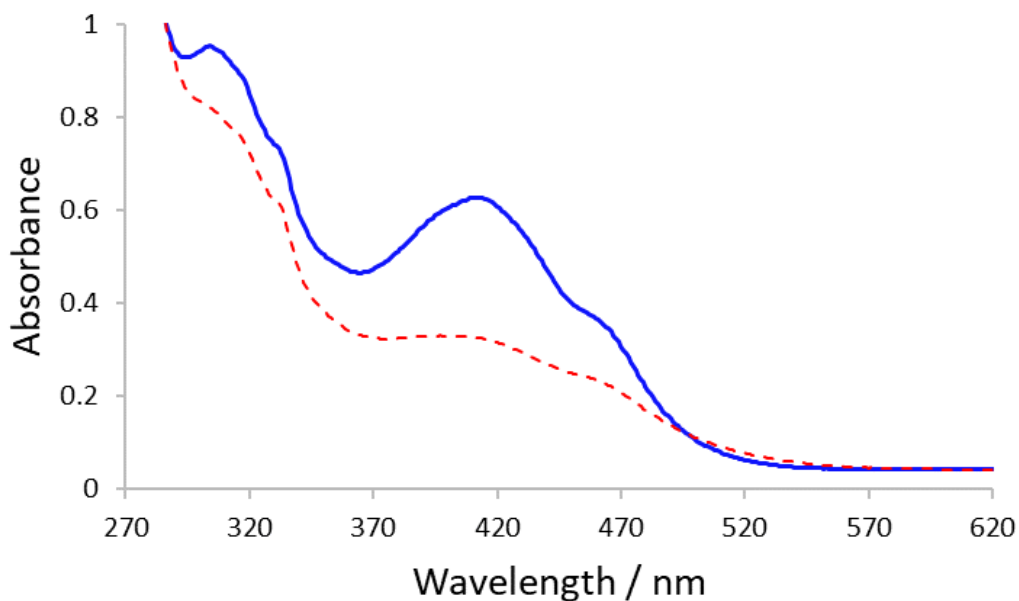


Figure S5. UV/Vis spectra of **1** before irradiation (shown in blue line) and at the photostationary state (PSS) (shown in the dashed red line) after irradiation at 365 nm for 10 min for the second time.

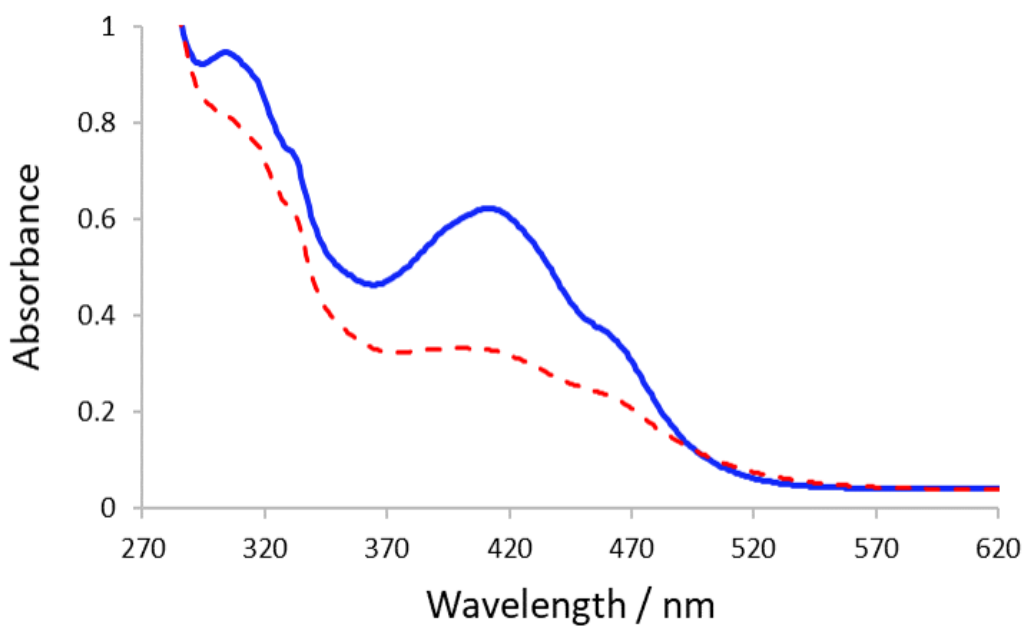


Figure S6. UV/Vis spectra of **1** before irradiation (shown in blue line) and at the photostationary state (PSS) (shown in the dashed red line) after irradiation at 365 nm for 10 min for the third time.

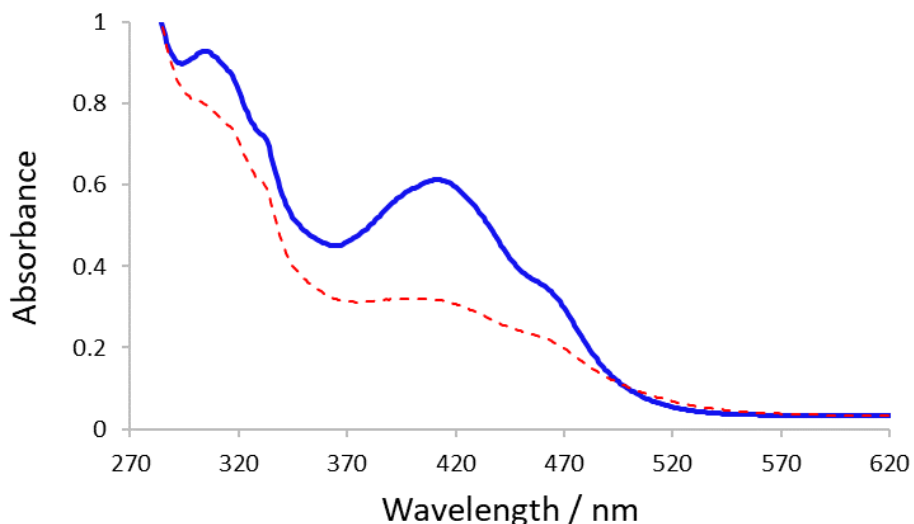


Figure S7. UV/Vis spectra of **1** before irradiation (shown in blue line) and at the photostationary state (PSS) (shown in the dashed red line) after irradiation at 365 nm for 10 min for the fourth time.

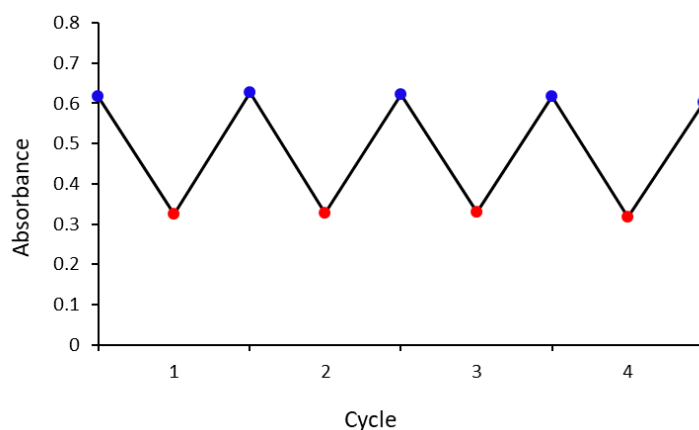


Figure S8. Light- and thermally-driven cycles of the *trans-cis* isomerisation of the azo bonds of **1**. Blue points correspond to **1** in the absence of application of irradiative conditions and red points correspond to the PSS obtained after irradiation at 365 nm for 10 min over four cycles.

Irradiation UV/Vis Spectroscopy Experimental Procedure

A 4.8×10^{-5} M acetonitrile solution of **1** was irradiated at 365 nm using a LED lamp source for 10 min and the temperature was kept at 298 K during irradiation. The photostationary state obtained after irradiation was measured at 298 K using an Aligent Cary 3500 UV/Vis photospectrometer fitted with a temperature control unit. The thermal *cis-trans* isomerisation process was monitored under non-irradiative conditions at 298 K using an Aligent Cary 3500 UV/Vis photospectrometer fitted with a temperature control unit.

Photoswitching Studies: CD Spectroscopy

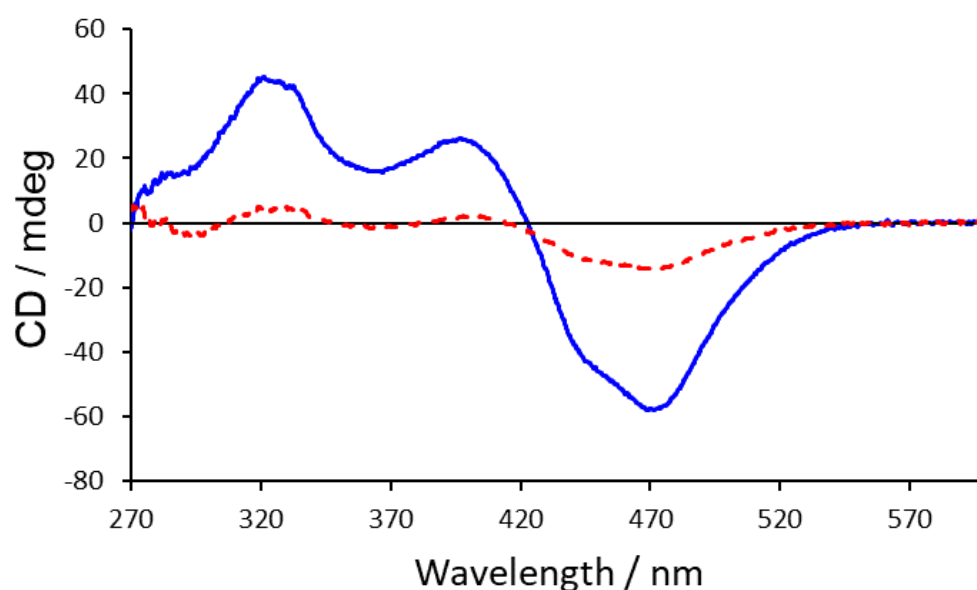


Figure S9. CD spectra of **1** before irradiation (shown in blue line) and at the photostationary state (PSS) (shown in the dashed red line) after irradiation of a 6.7×10^{-5} M acetonitrile solution at 365 nm for 10 min for the first time.

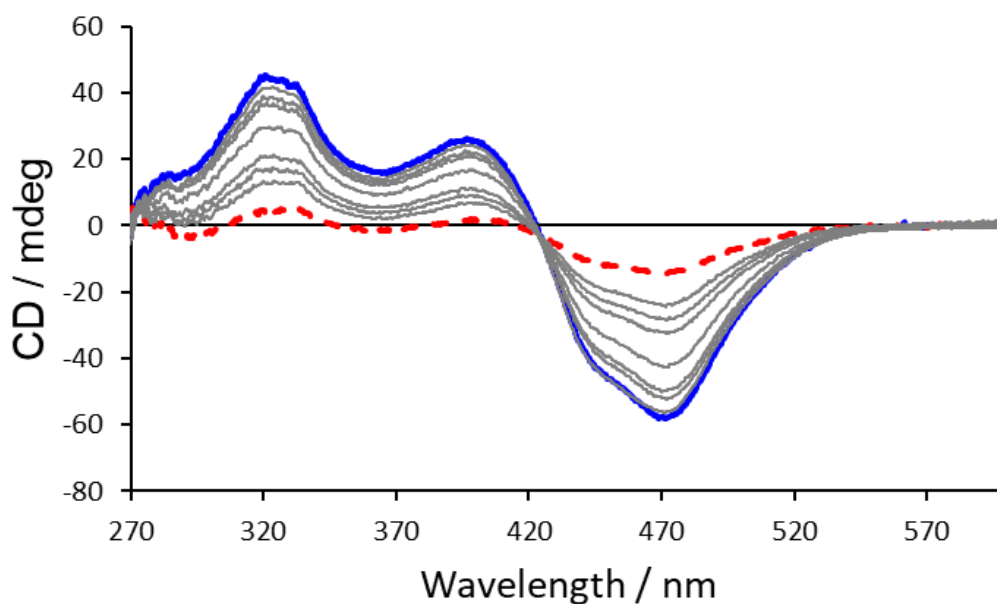


Figure S10. UV/Vis spectra of **1** before irradiation (shown in blue line) and at the photostationary state (PSS) (shown in the dashed red line) after irradiation of a 6.7×10^{-5} M acetonitrile solution at 365 nm for 10 min. Grey lines represent spectra taken between PSS and up to 230 min after irradiation.

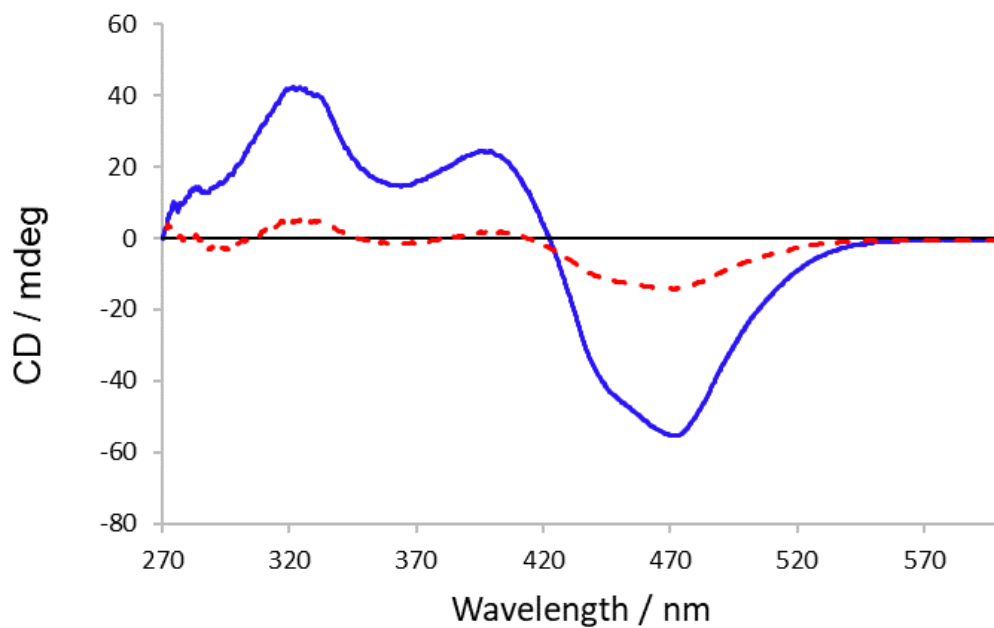


Figure S11. CD spectra of **1** before irradiation (shown in blue line) and at the photostationary state (PSS) (shown in the dashed red line) after irradiation of a 6.7×10^{-5} M acetonitrile solution at 365 nm for 10 min for the second time.

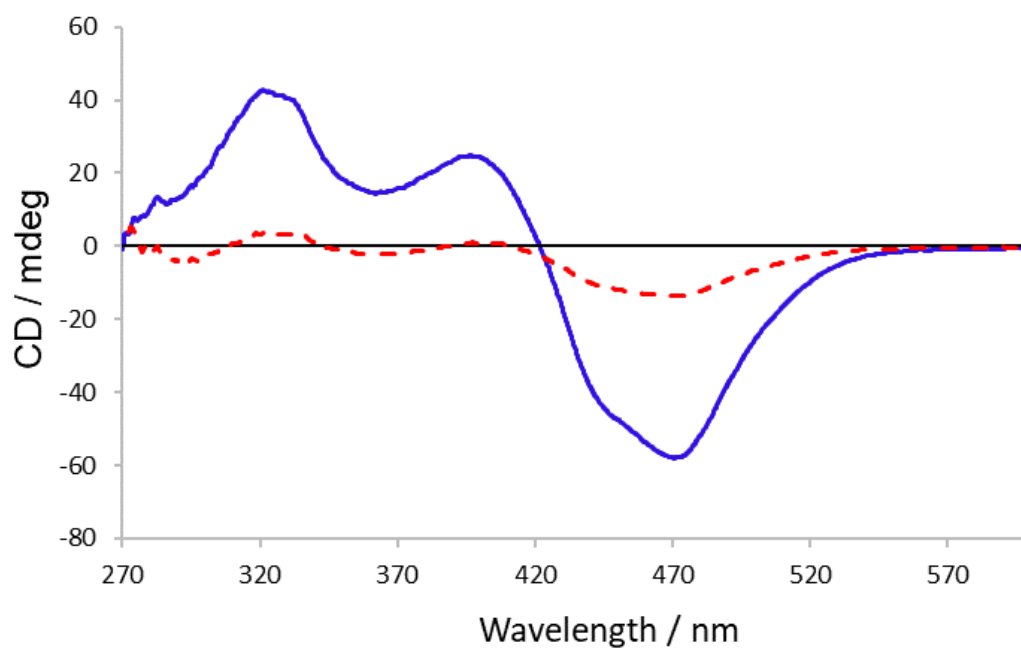


Figure S12. CD spectra of **1** before irradiation (shown in blue line) and at the photostationary state (PSS) (shown in the dashed red line) after irradiation of a 6.7×10^{-5} M acetonitrile solution at 365 nm for 10 min for the third time.

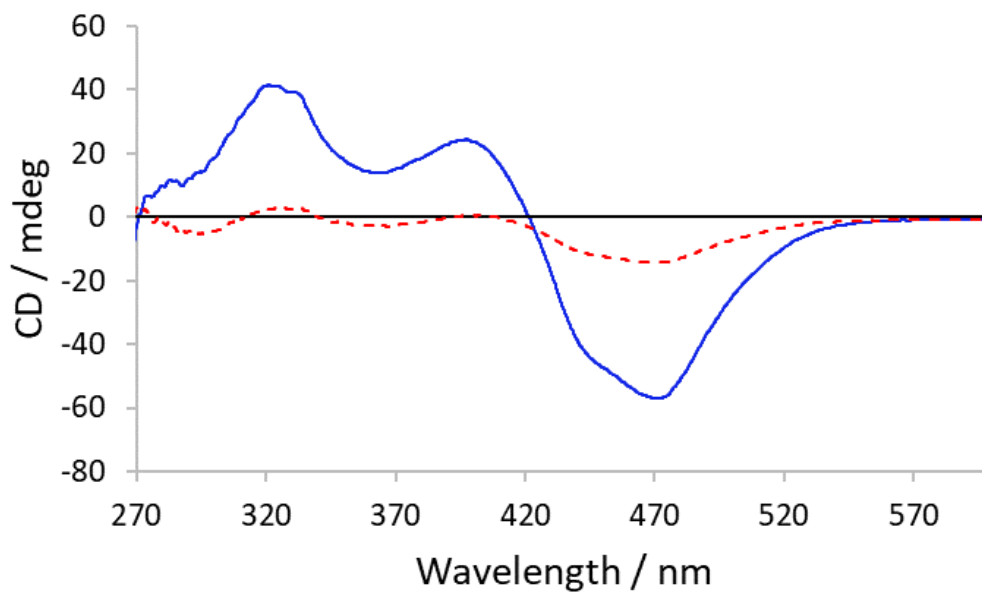


Figure S13. CD spectra of **1** before irradiation (shown in blue line) and at the photostationary state (PSS) (shown in the dashed red line) after irradiation of a 6.7×10^{-5} M acetonitrile solution at 365 nm for 10 min for the fourth time.

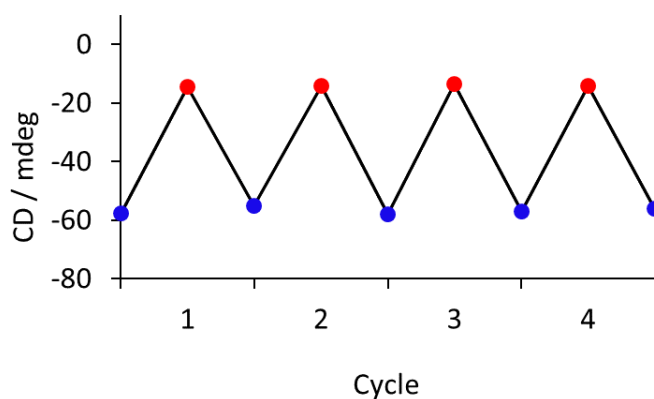


Figure S14. Light- and thermally-driven cycles of the *trans-cis* isomerisation of the azo bonds of **1**. Blue points correspond to **1** in the absence of application of irradiative conditions and red points correspond to the PSS obtained at 472 nm after irradiation of a 6.7×10^{-5} M acetonitrile solution of **1** at 365 nm for 10 min over four cycles.

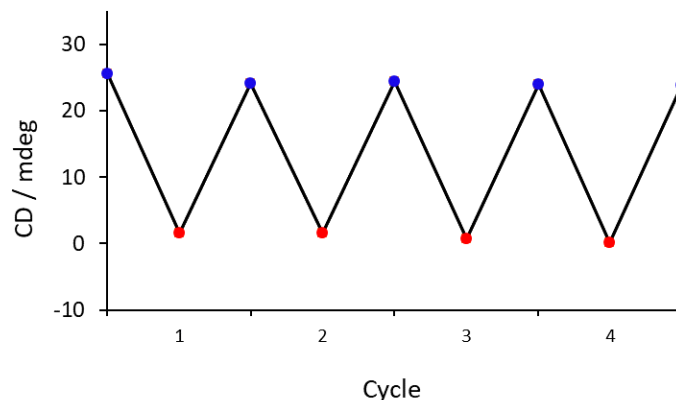


Figure S15. Light- and thermally-driven cycles of the *trans-cis* isomerisation of the azo bonds of **1**. Blue points correspond to **1** in the absence of application of irradiative conditions and red points correspond to the PSS obtained at 394 nm after irradiation of a 6.7×10^{-5} M acetonitrile solution of **1** at 365 nm for 10 min over four cycles.

Irradiation CD Spectroscopy Experimental Procedure

A 6.7×10^{-5} mM acetonitrile solution of **1** was irradiated at 365 nm using a LED lamp source for 10 min and the temperature was kept at 298 K during irradiation. The photostationary state obtained after irradiation was measured on a Jasco J-715 spectropolarimeter at 298 K. The thermal *cis-trans* isomerisation process was monitored under non-irradiative conditions using a Jasco J-715 spectropolarimeter.

Photoswitching Studies: ^1H NMR Spectroscopy

i) Irradiation for 1st Time

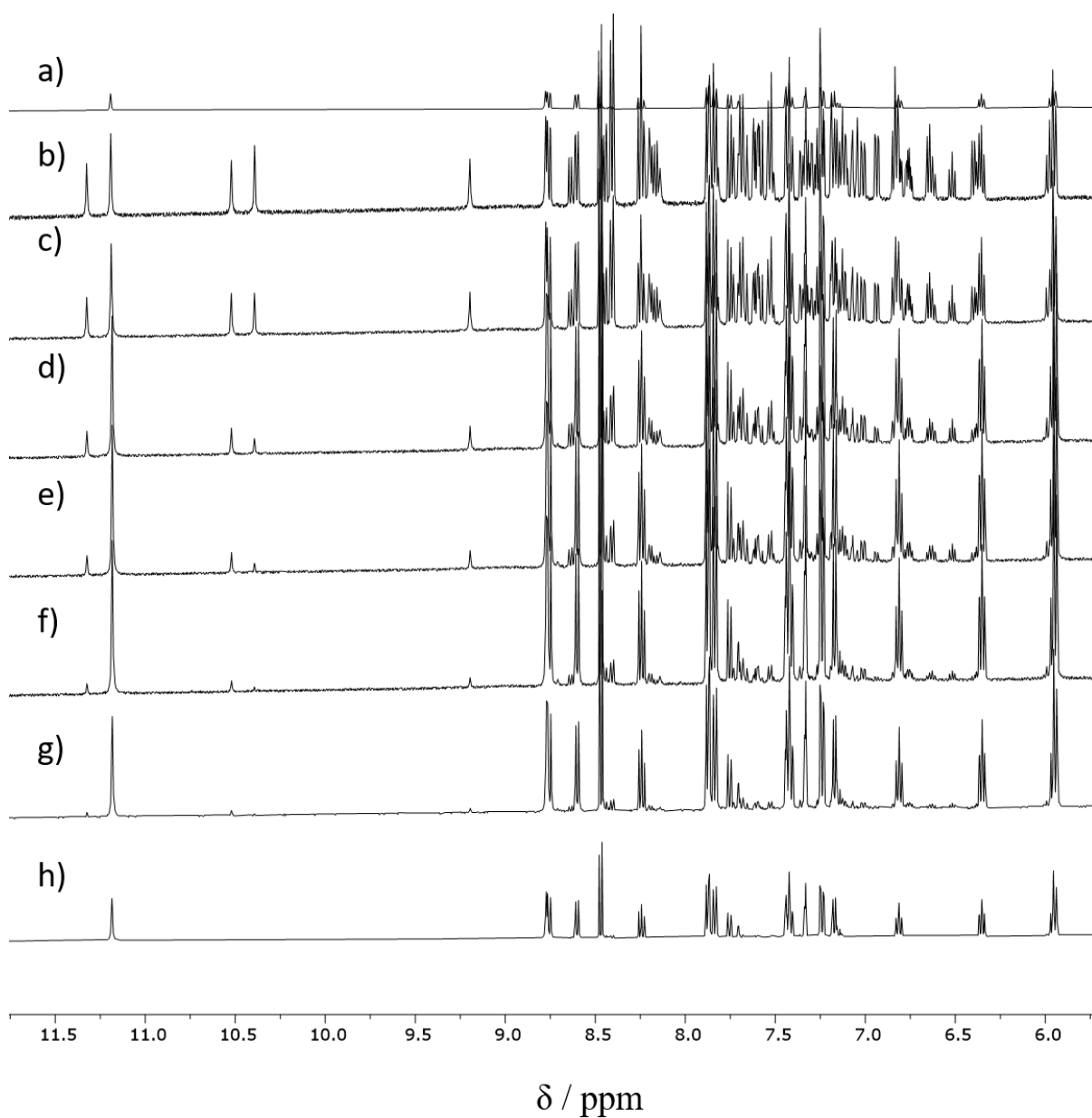


Figure S16. ^1H NMR spectra of **1** (400 MHz, CD_3CN , 295 K) a) before irradiation, b) PSS after 1st treatment with 45 min irradiation at 365 nm, c) 45 min after irradiation, d) 105 min after irradiation, e) 135 min after irradiation, f) 195 min after irradiation, g) 225 min after irradiation and h) 285 min after irradiation.

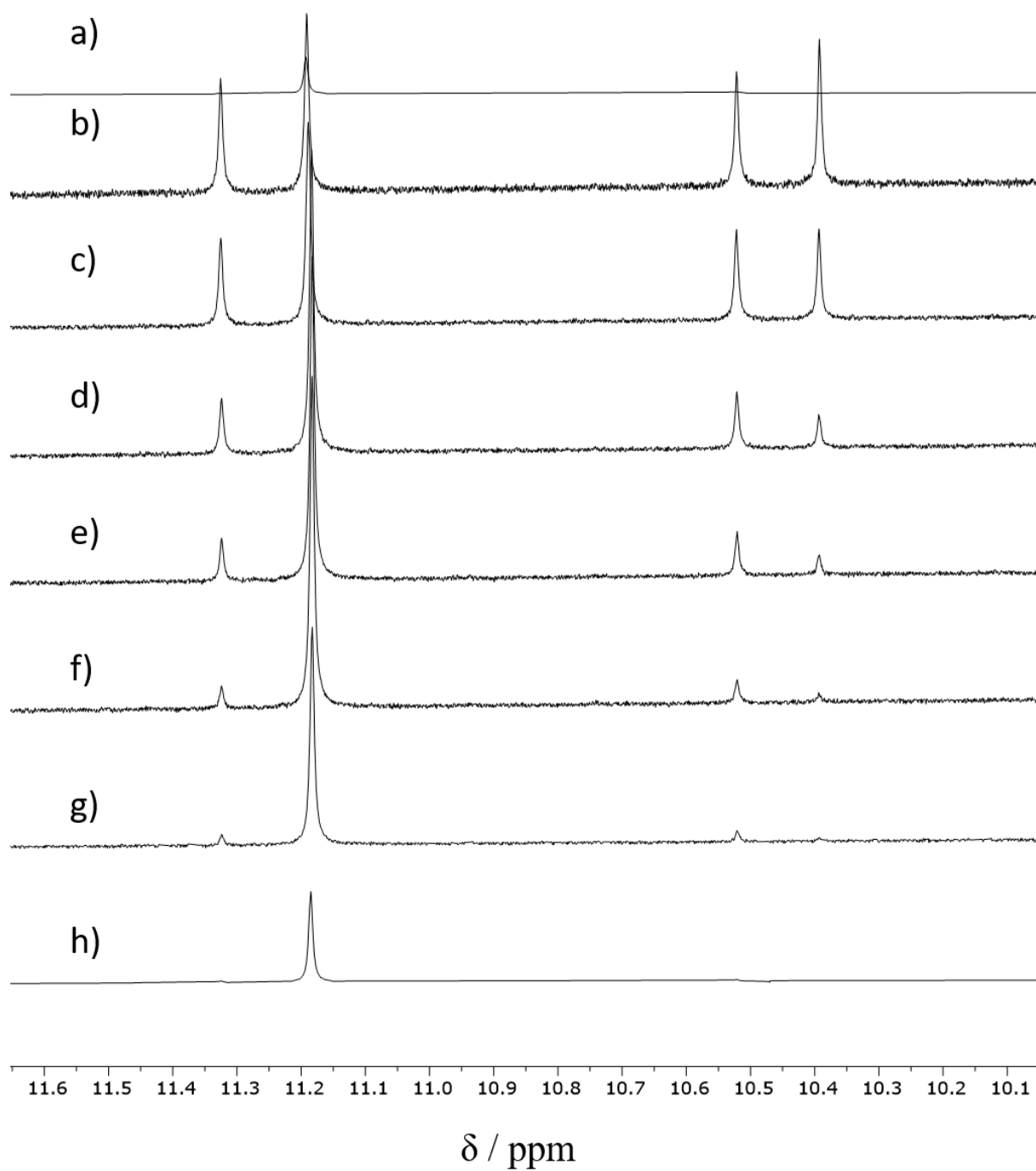


Figure S17. Partial ¹H NMR spectra of **1** (400 MHz, CD₃CN, 295 K) a) before irradiation, b) PSS after 1st treatment with 45 min irradiation at 365 nm, c) 45 min after irradiation, d) 105 min after irradiation, e) 135 min after irradiation, f) 195 min after irradiation, g) 225 min after irradiation and h) 285 min after irradiation.

ii) Irradiation for 2nd Time

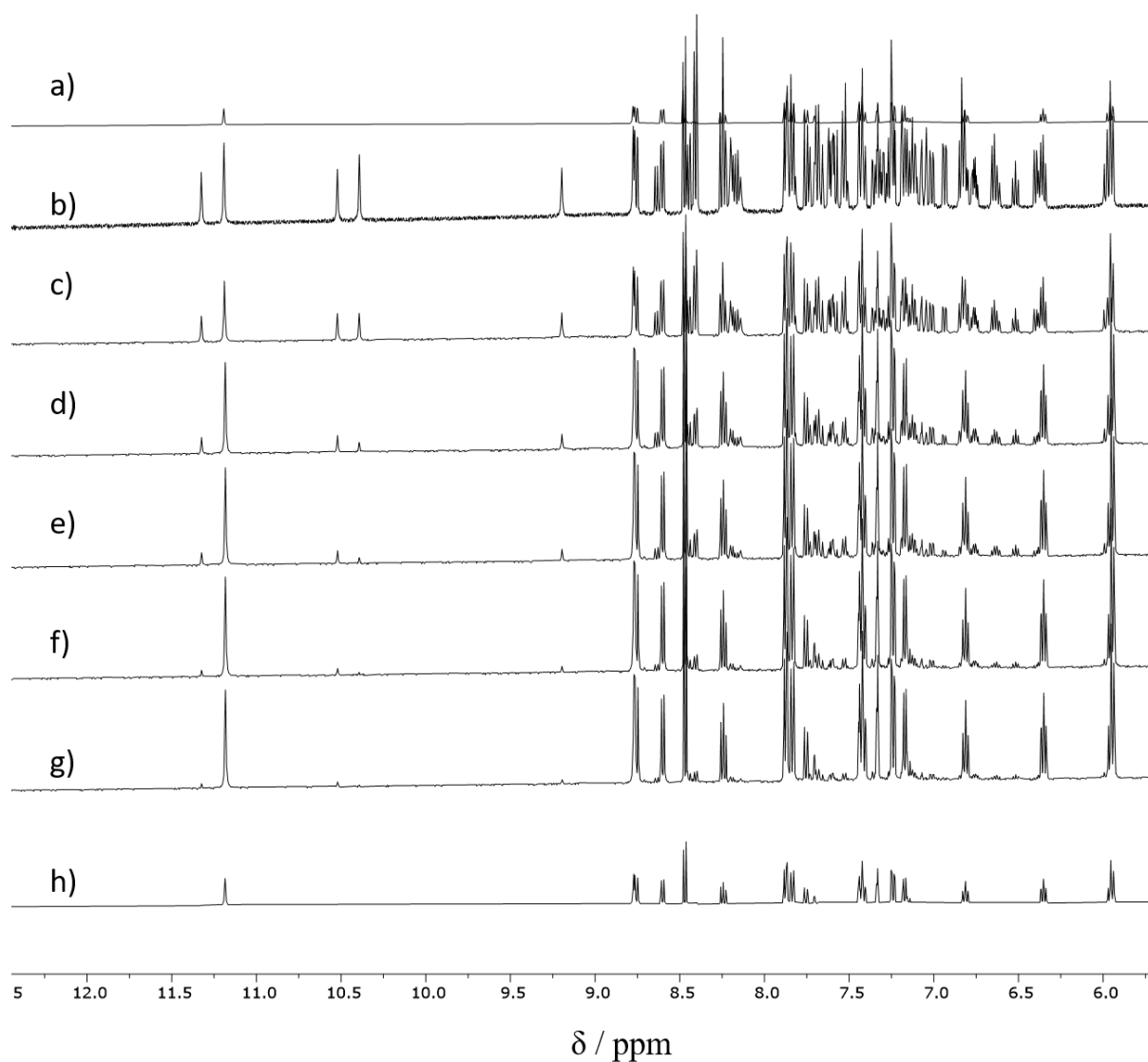


Figure S18. ¹H NMR spectra of **1** (400 MHz, CD₃CN, 295 K) a) before irradiation, b) PSS after 2nd treatment with 45 min irradiation at 365 nm, c) 45 min after irradiation, d) 75 min after irradiation, e) 105 min after irradiation, f) 155 min after irradiation, g) 185 min after irradiation at 365 nm and h) 285 min after irradiation.

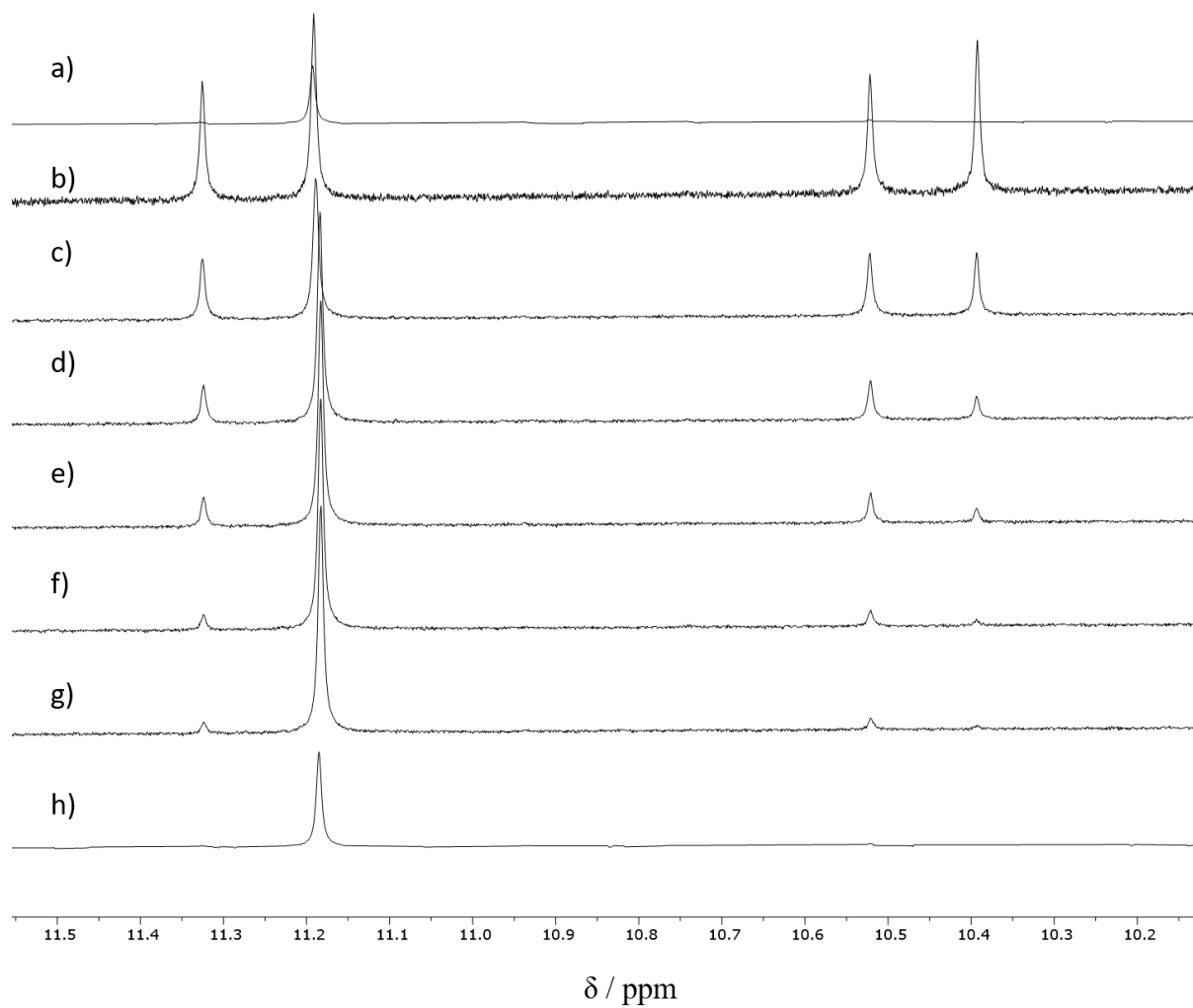


Figure S19. Partial ^1H NMR spectra of **1** (400 MHz, CD_3CN , 295 K) a) before irradiation, b) PSS after 2nd treatment with 45 min irradiation at 365 nm, c) 45 min after irradiation, d) 75 min after irradiation, e) 105 min after irradiation, f) 155 min after irradiation, g) 185 min after irradiation at 365 nm and h) 285 min after irradiation.

iii) Irradiation for 3rd Time

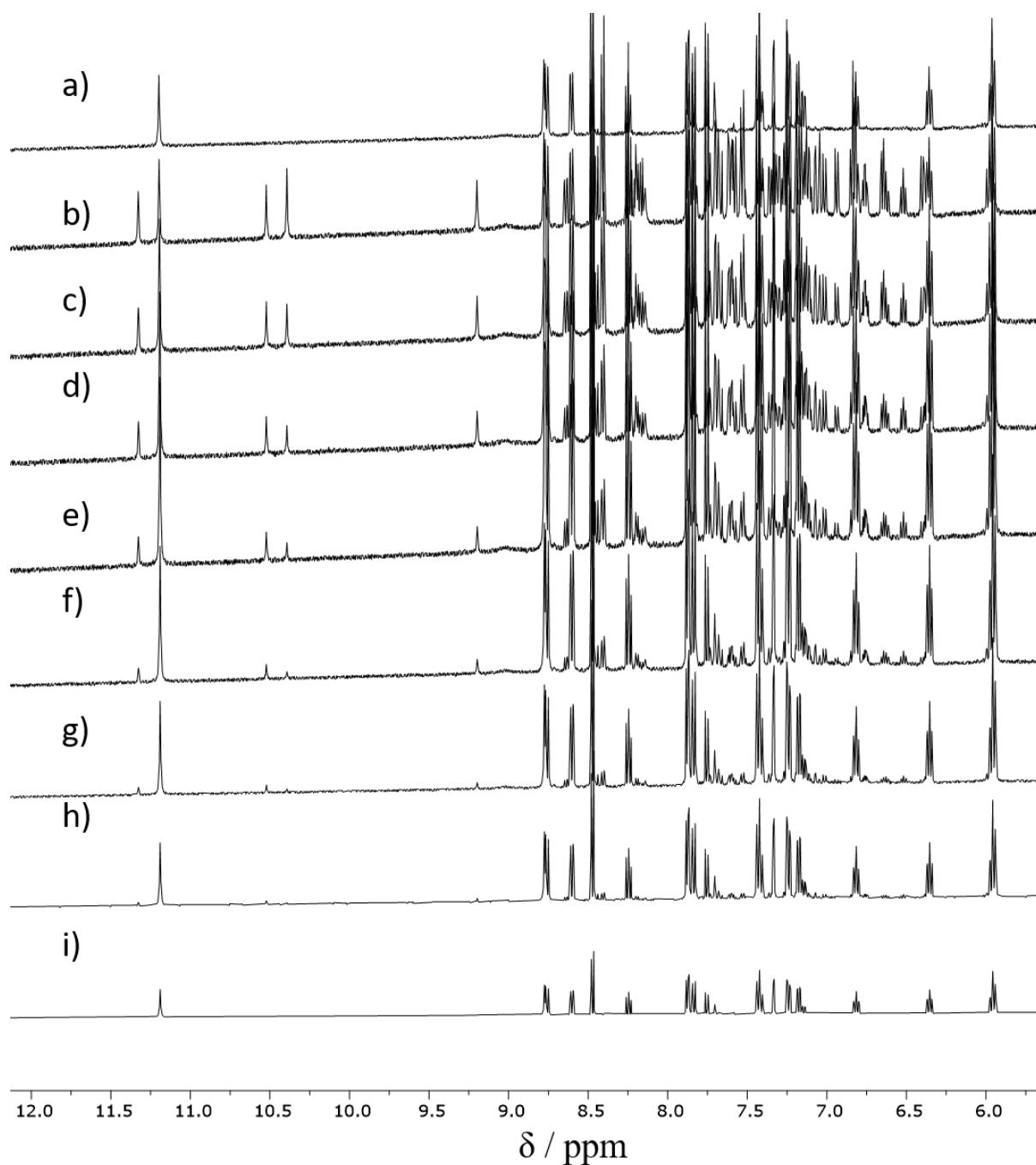


Figure S20. ¹H NMR spectra of **1** (400 MHz, CD₃CN, 295 K) a) before irradiation, b) PSS after 3rd treatment with 45 min irradiation at 365 nm, c) 30 min after irradiation, d) 60 min after irradiation, e) 90 min after irradiation, f) 120 min after irradiation, g) 180 min after irradiation, h) 225 min after irradiation and i) 285 min after irradiation.

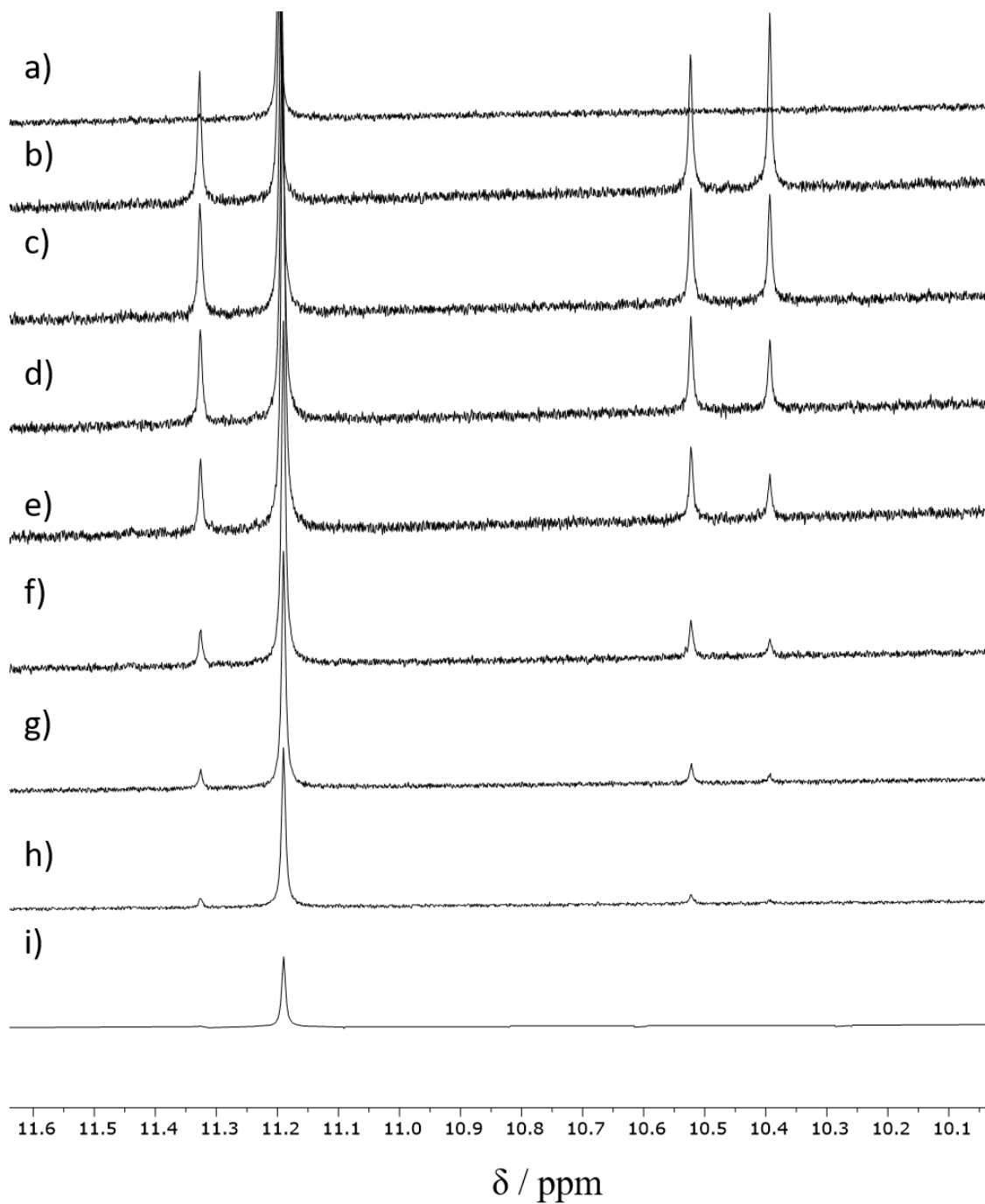


Figure S21. Partial ^1H NMR spectra of **1** (400 MHz, CD_3CN , 295 K) a) before irradiation, b) PSS after 3rd treatment with 45 min irradiation at 365 nm, c) 30 min after irradiation, d) 60 min after irradiation, e) 90 min after irradiation, f) 120 min after irradiation, g) 180 min after irradiation, h) 225 min after irradiation and i) 285 min after irradiation.

iv) Irradiation for 4th Time

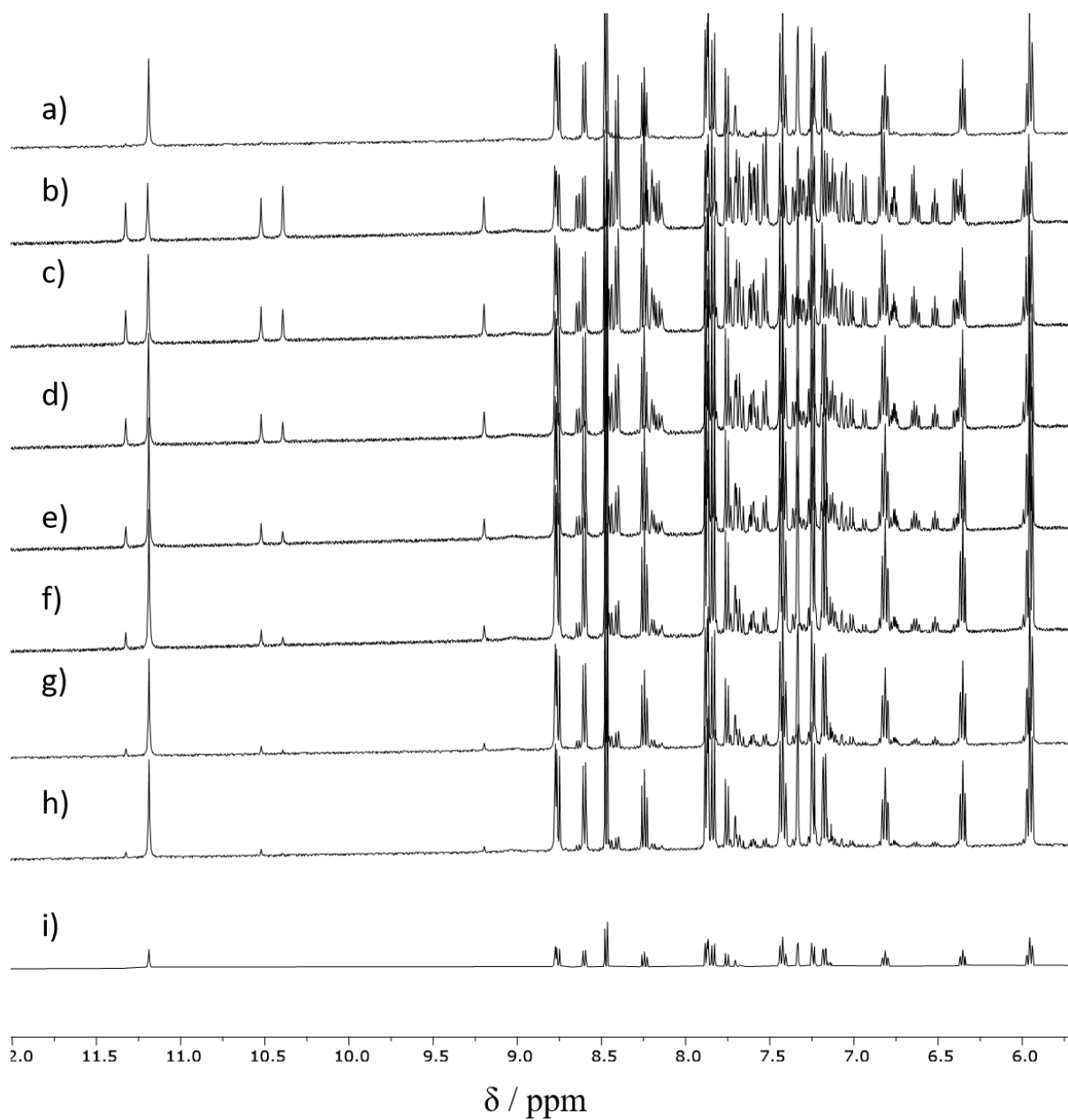


Figure S22. ¹H NMR spectra of **1** (400 MHz, CD₃CN, 295 K) a) before irradiation, b) PSS after 4th treatment with 45 min irradiation at 365 nm, c) 30 min after irradiation, d) 60 min after irradiation, e) 90 min after irradiation, f) 140 min after irradiation, g) 170 min after irradiation, h) 220 min after irradiation and i) 285 min after irradiation.

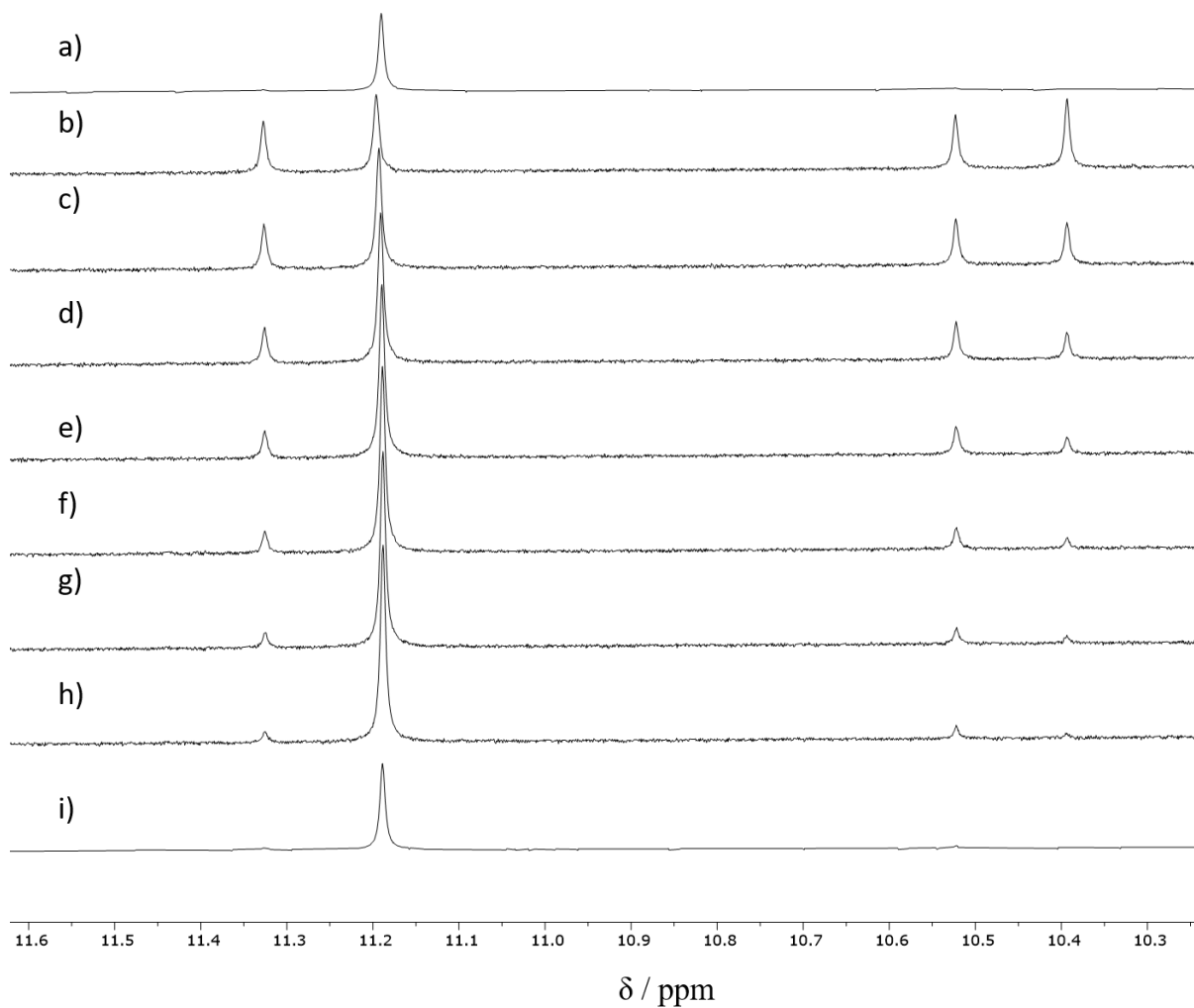


Figure S23. Partial ¹H NMR spectra of **1** (400 MHz, CD₃CN, 295 K) a) before irradiation, b) PSS after 4th treatment with 45 min irradiation at 365 nm, c) 30 min after irradiation, d) 60 min after irradiation, e) 90 min after irradiation, f) 140 min after irradiation, g) 170 min after irradiation, h) 220 min after irradiation and i) 285 min after irradiation.

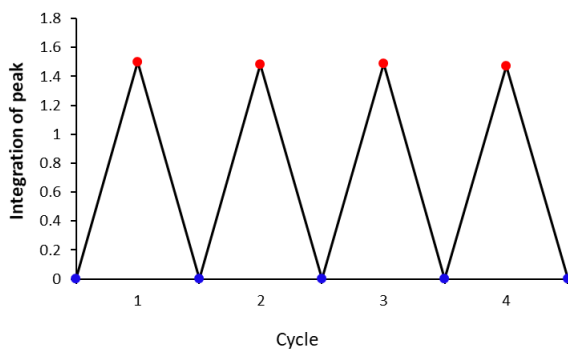


Figure S24. Light- and thermally-driven cycles of the trans-cis isomerisation of the azo bonds of **1**. Blue points correspond to **1** in the absence of the application of irradiative conditions and red points correspond to the PSS obtained for the NHs of the central pyridylcarboxamide unit of the *Z/Z* isomer of **1** after irradiation of a 1.1 mM acetonitrile solution with 365 nm for 45 over four cycles. Integration of the area under the peak corresponding to the Hc proton (NH of the central pyridylcarboxamide unit) in the *Z/Z* isomer of **1**.

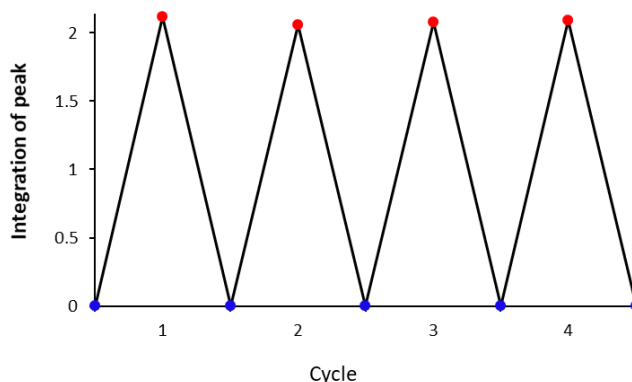


Figure S25. Light- and thermally-driven cycles of the trans-cis isomerisation of the azo bonds of **1**. Blue points correspond to **1** in the absence of the application of irradiative conditions and red points correspond to the PSS obtained for the NHs of the central pyridylcarboxamide unit of the *E/Z* isomer of **1** after irradiation of a 1.1 mM acetonitrile solution with 365 nm for 45 over four cycles. Integration of the area under the peaks corresponding to the NHs of the central pyridylcarboxamide unit in the *E/Z* isomer of **1**.

Irradiation NMR Spectroscopy Experimental Procedure

A 1.1 mM acetonitrile solution of **1** was irradiated at 365 nm using a LED lamp source for 45 min and the temperature was kept at 298 K during irradiation. The photostationary state obtained after irradiation was measured at 298 K using a Bruker AV4-500 MHz NMR spectrometer. The thermal *cis-trans* isomerisation process was monitored under non-irradiative conditions using a Bruker AV4-500 MHz NMR spectrometer at 298 K.

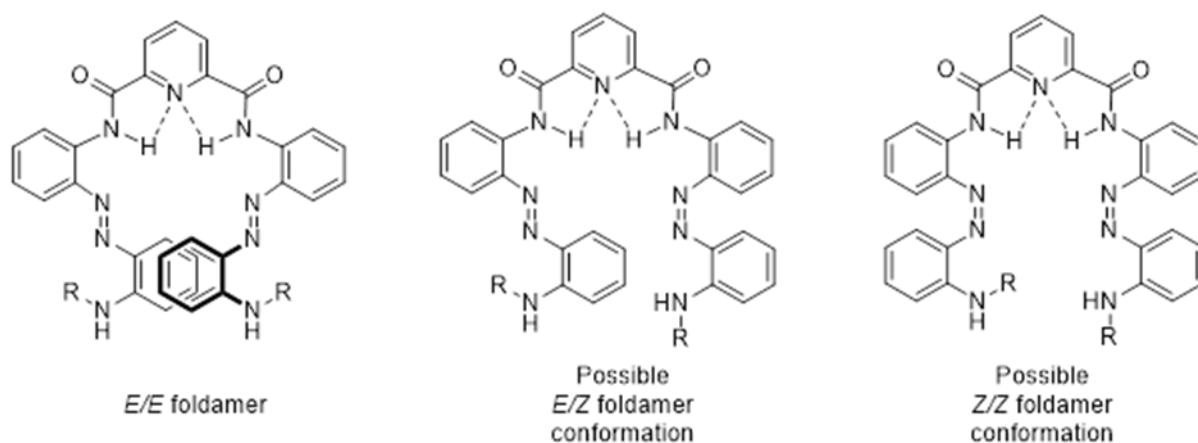


Figure S26. Figure showing three different conformations of 1 that can be adopted upon the application of irradiative conditions.

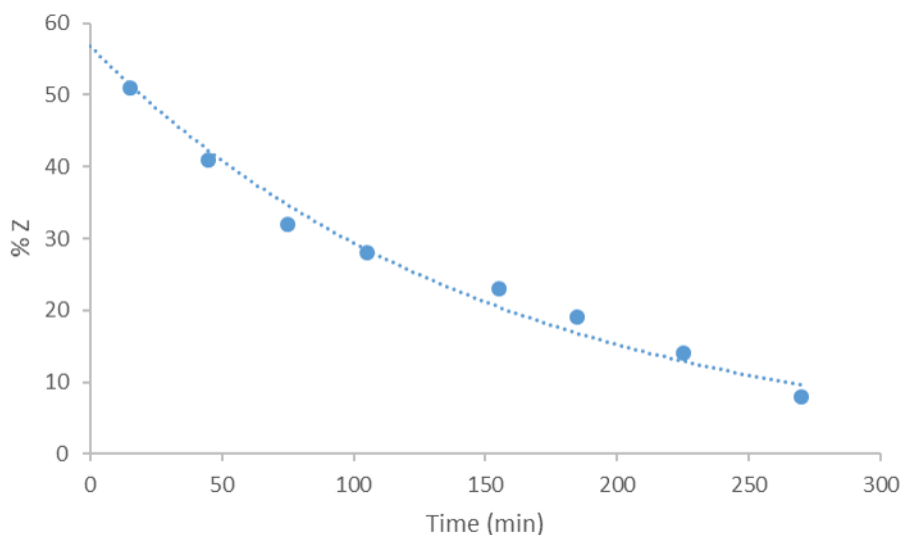


Figure S27. Lifetime plot of Z-1 based on ^1H NMR integration of NHs of the central pyridylcarboxamide unit over time at 298 K in MeCN-d_3 . Exponential decay model was used to determine t_1 (Equation S1). Half-life ($t_{1/2}$) was determined using Equation S2.

$$y = A_1 e^{(-x/t_1)} \quad (\text{Equation S1})$$

$$T_{1/2} = t_1 \ln 2 \quad (\text{Equation S2})$$

Aggregation Studies: ^1H NMR Spectroscopy

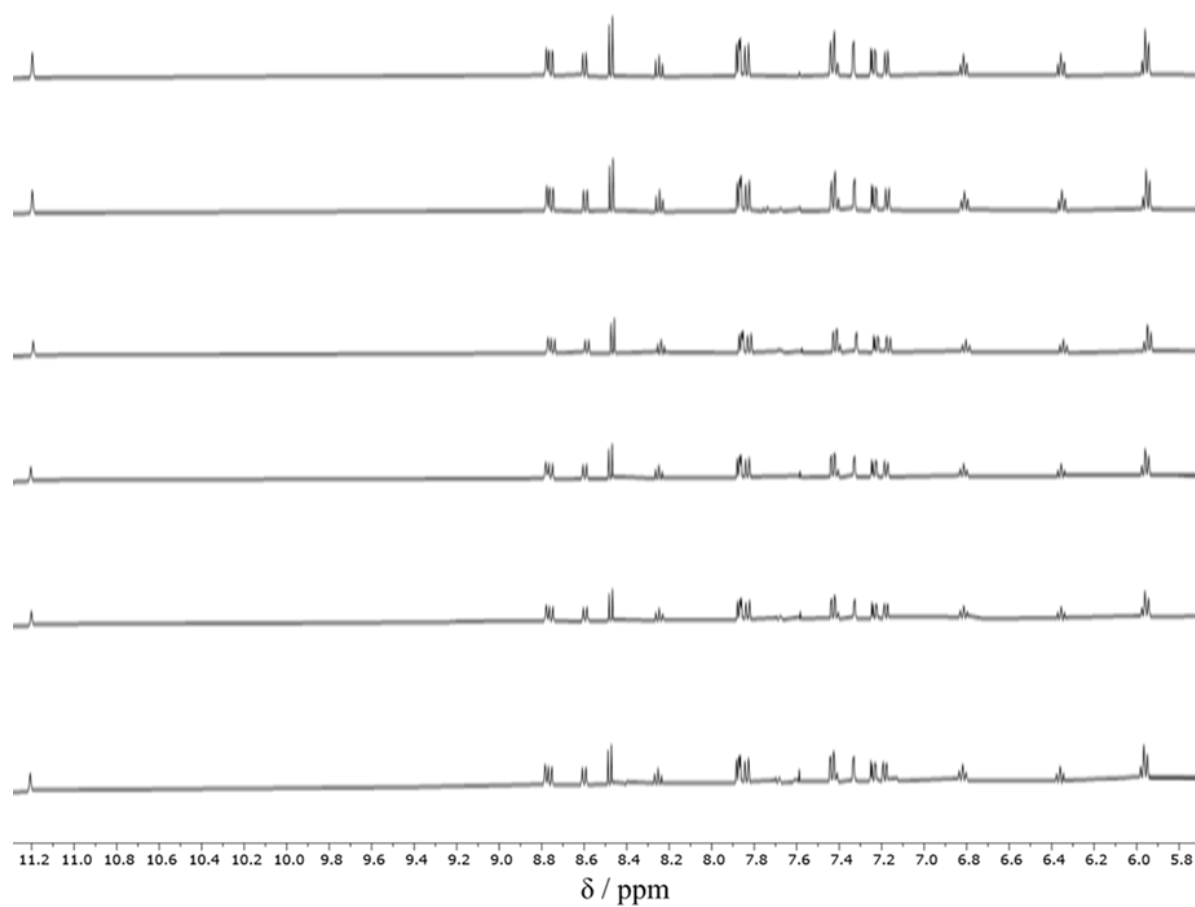


Figure S28. Stack plot of partial ^1H NMR spectra of **1** (400 MHz, CD_3CN , 298 K) taken at varying concentrations: a) 1.7 mM, b) 1.0 mM, c) 0.8 mM, d) 0.4 mM, e) 0.3 mM

Crystal Data and Structural Refinement

a) 1

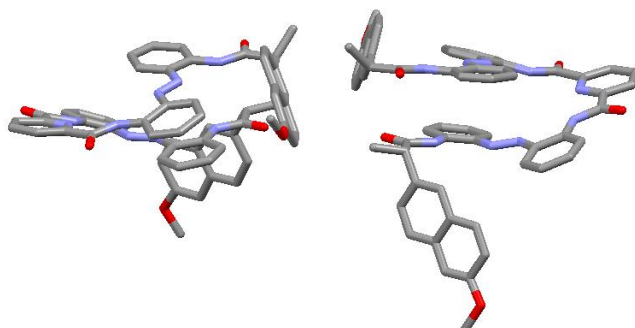
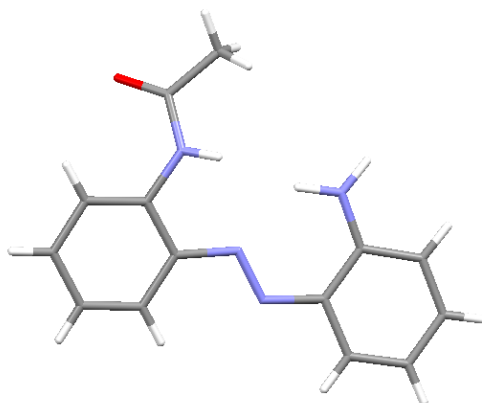


Table 1 Crystal data and structure refinement for 1.

Identification code	1
Empirical formula	C _{60.5} H _{50.5} Cl _{4.5} N ₉ O ₆
Formula weight	1159.12
Temperature/K	100.00(10)
Crystal system	triclinic
Space group	<i>P</i> 1
<i>a</i> /Å	10.3827(3)
<i>b</i> /Å	15.5971(4)
<i>c</i> /Å	19.3486(6)
α /°	68.486(3)
β /°	74.716(3)
γ /°	88.134(2)
Volume/Å ³	2804.72(15)
<i>Z</i>	2
ρ_{calc} /cm ³	1.373
μ /mm ⁻¹	2.634
<i>F</i> (000)	1202.0
Crystal size/mm ³	0.34 × 0.07 × 0.025
Radiation	Cu K α (λ = 1.54178)
2 θ range for data collection/°	5.1 to 136.906
Index ranges	-12 ≤ <i>h</i> ≤ 11, -18 ≤ <i>k</i> ≤ 18, -23 ≤ <i>l</i> ≤ 23
Reflections collected	30674
Independent reflections	30674 [<i>R</i> _{int} = ?, <i>R</i> _{sigma} = 0.0186]
Data/restraints/parameters	30674/202/1548
Goodness-of-fit on <i>F</i> ²	1.016
Final <i>R</i> indexes [<i>I</i> ≥ 2 σ (<i>I</i>)]	<i>R</i> ₁ = 0.0627, <i>wR</i> ₂ = 0.1733
Final <i>R</i> indexes [all data]	<i>R</i> ₁ = 0.0661, <i>wR</i> ₂ = 0.1767
Largest diff. peak/hole / e Å ⁻³	0.57/-0.45
Flack parameter	0.019(11)

b) 4**Table 2 Crystal data and structure refinement for 4.**

Identification code	4
Empirical formula	C ₁₄ H ₁₄ N ₄ O
Formula weight	254.29
Temperature/K	100.01(10)
Crystal system	orthorhombic
Space group	<i>P</i> 2 ₁ 2 ₁ 2 ₁
<i>a</i> /Å	4.7704(2)
<i>b</i> /Å	9.7654(4)
<i>c</i> /Å	26.4117(12)
α /°	90
β /°	90
γ /°	90
Volume/Å ³	1230.39(9)
<i>Z</i>	4
ρ_{calc} /cm ³	1.373
μ /mm ⁻¹	0.736
<i>F</i> (000)	536.0
Crystal size/mm ³	0.292 × 0.075 × 0.051
Radiation	Cu K α (λ = 1.54184)
2 θ range for data collection/°	9.656 to 146.238
Index ranges	-5 ≤ <i>h</i> ≤ 5, -12 ≤ <i>k</i> ≤ 12, -32 ≤ <i>l</i> ≤ 32
Reflections collected	11654
Independent reflections	2424 [<i>R</i> _{int} = 0.0413, <i>R</i> _{sigma} = 0.0266]
Data/restraints/parameters	2424/0/185
Goodness-of-fit on <i>F</i> ²	1.061
Final <i>R</i> indexes [<i>I</i> ≥ 2 σ (<i>I</i>)]	<i>R</i> ₁ = 0.0388, <i>wR</i> ₂ = 0.0969
Final <i>R</i> indexes [all data]	<i>R</i> ₁ = 0.0403, <i>wR</i> ₂ = 0.0982
Largest diff. peak/hole / e Å ⁻³	0.34/-0.19
Flack parameter	0.21(16)

Solid State Analysis of 1

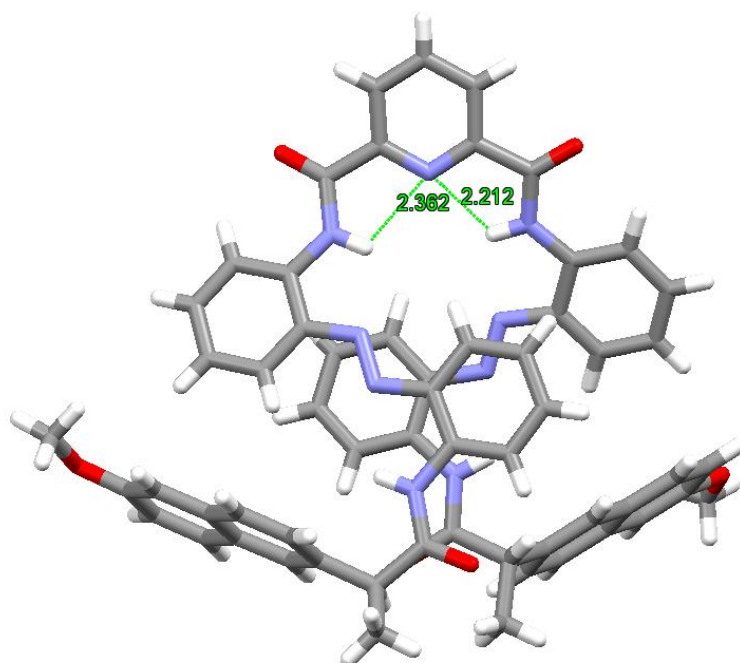


Figure S29. Solid state analysis of one molecule of **1** in the unit cell highlighting the presence of bifurcated⁷ intramolecular N-H \cdots N hydrogen bonding interactions involving the N atom of the pyridine and the two NH's of the adjacent amide bonds leading to the *syn-syn* conformation about the central pyridinecarboxamide unit.⁸

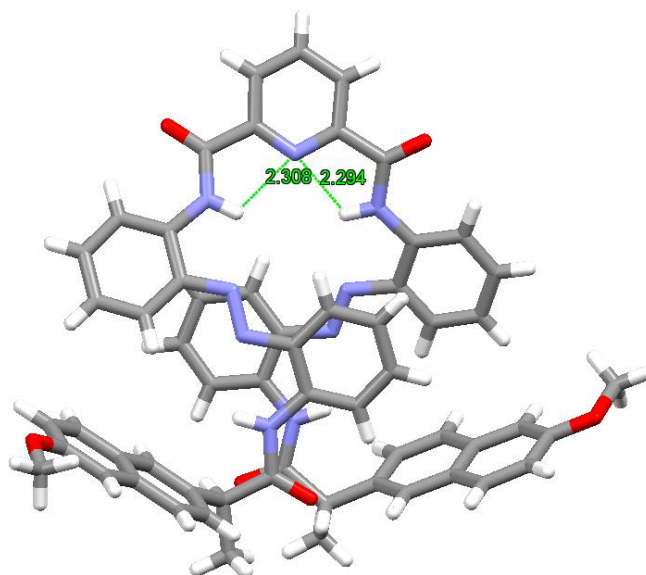


Figure S30. Solid state analysis of one molecule of **1** in the unit cell highlighting the presence of bifurcated⁷ intramolecular N-H \cdots N hydrogen bonding interactions involving the N atom of the pyridine and the two NH's of the adjacent amide bonds leading to the *syn-syn* conformation about the central pyridinecarboxamide unit.⁸

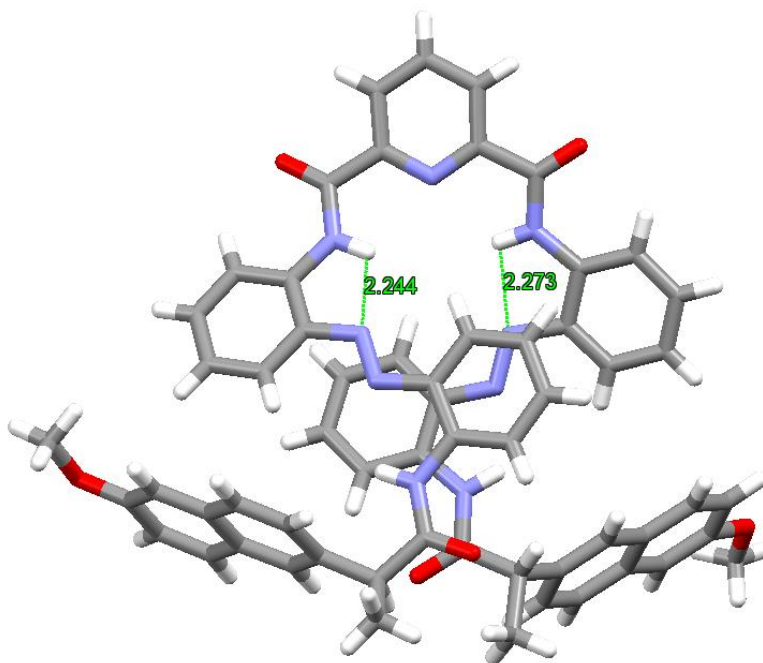


Figure S31. Solid state analysis of one molecule in the unit cell of **1** highlighting the close contacts between the pyridyl amide NHs and the adjacent azo N atoms.⁹

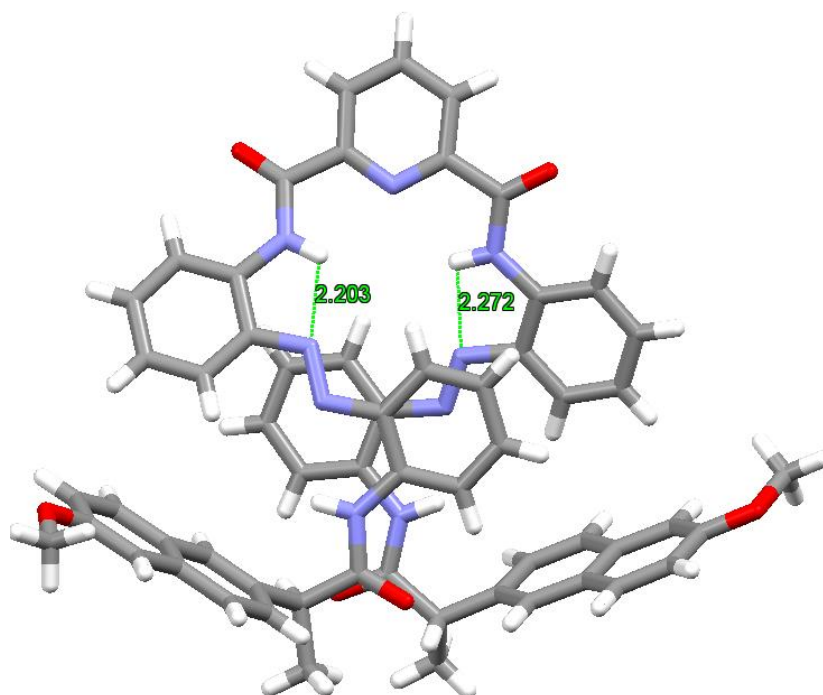


Figure S32. Solid state analysis of one molecules in the unit cell of **1** highlighting the close contacts between the pyridyl amide NHs and the adjacent azo N atoms.⁹

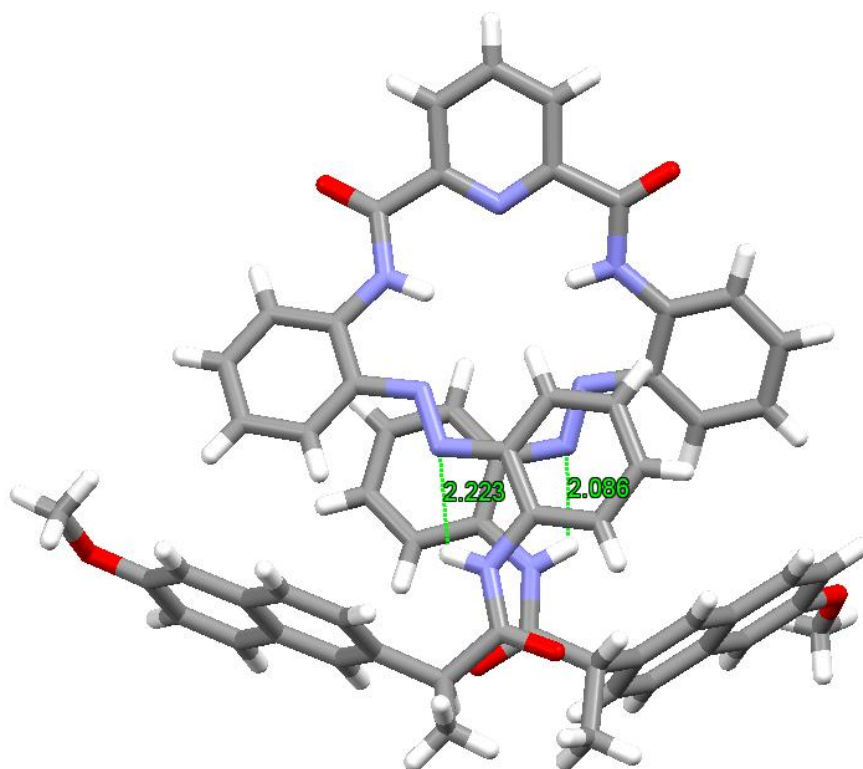


Figure S33. Solid state analysis of one of the molecules in the unit cell of **1** highlighting the close contacts between the terminal acetyl amide and the adjacent azo N atoms.⁹

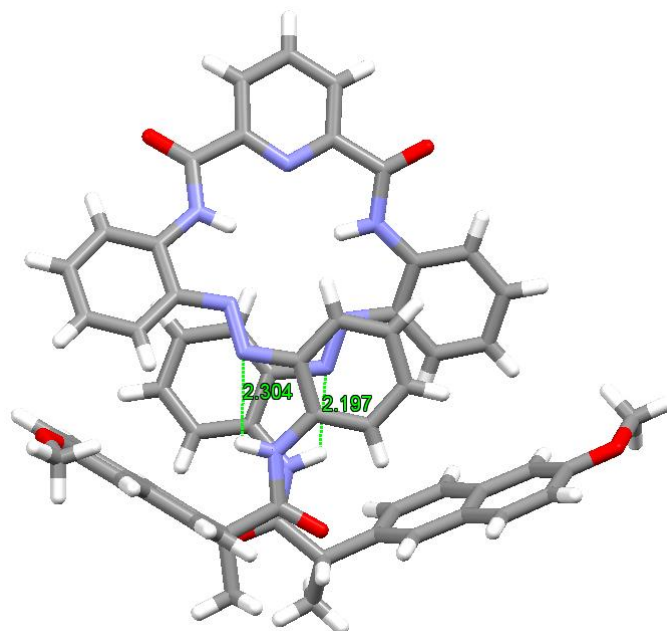


Figure S34. Solid state analysis of one of the molecules in the unit cell of **1** highlighting the close contacts between the terminal acetyl amide and the adjacent azo N atoms.⁹

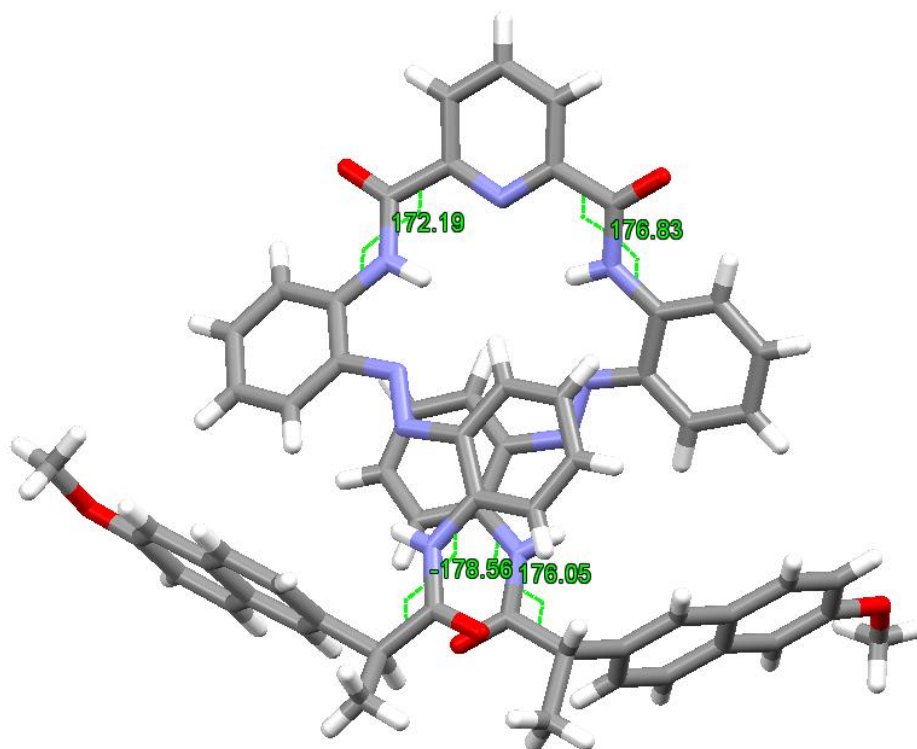


Figure S35. Solid state analysis of one of the molecules in the unit cell of **1** highlighting the torsion angles of the internal and terminal peptide bonds.

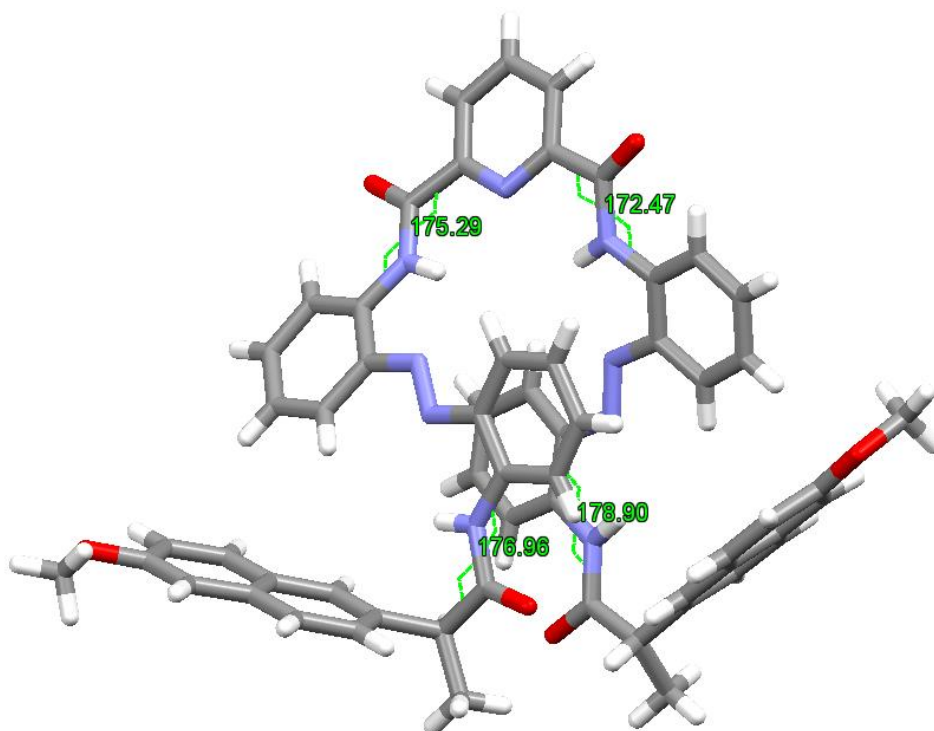


Figure S36. Solid state analysis of one of the molecules in the unit cell of **1** highlighting the torsion angles of the internal and terminal peptide bonds.

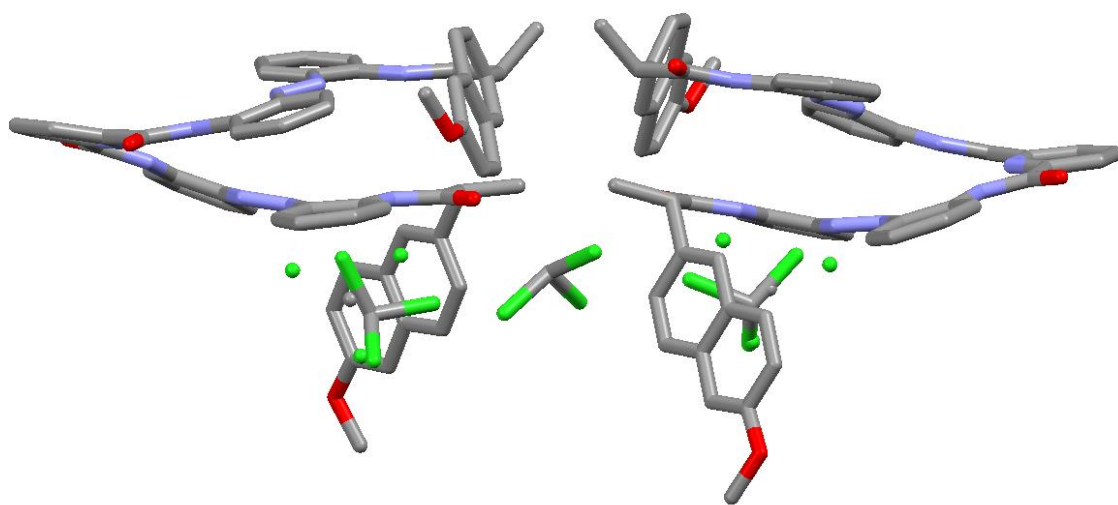


Figure S37. Solid state analysis of **1** highlighting the two distinct molecules of **1** of the same handedness in the unit cell and the presence of three chloroform solvent molecules and two disordered chloroform solvent molecules.

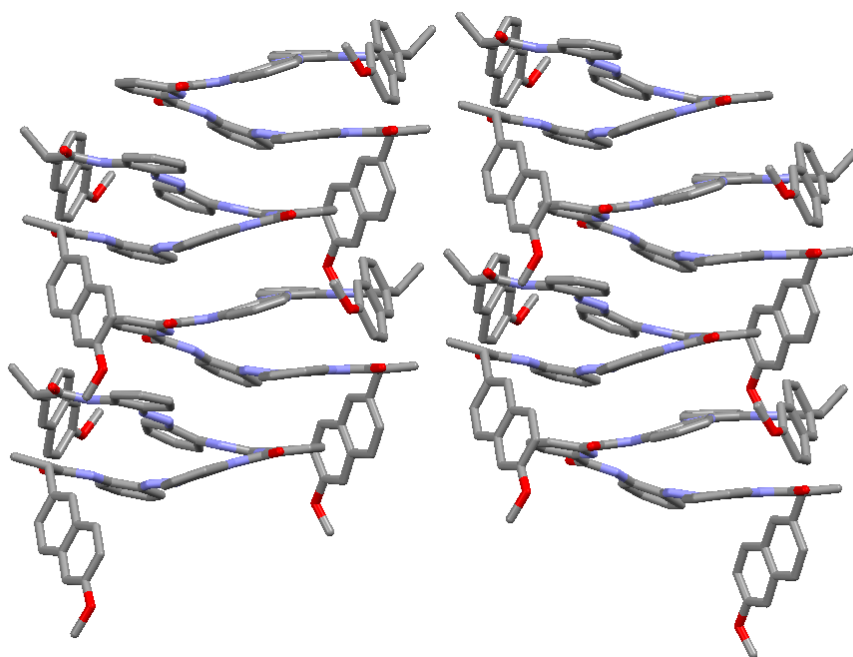


Figure S38. Solid state analysis of **1** highlighting the crystal packing; showing the presence of columnar stacks of molecules of the same helical screw-sense.

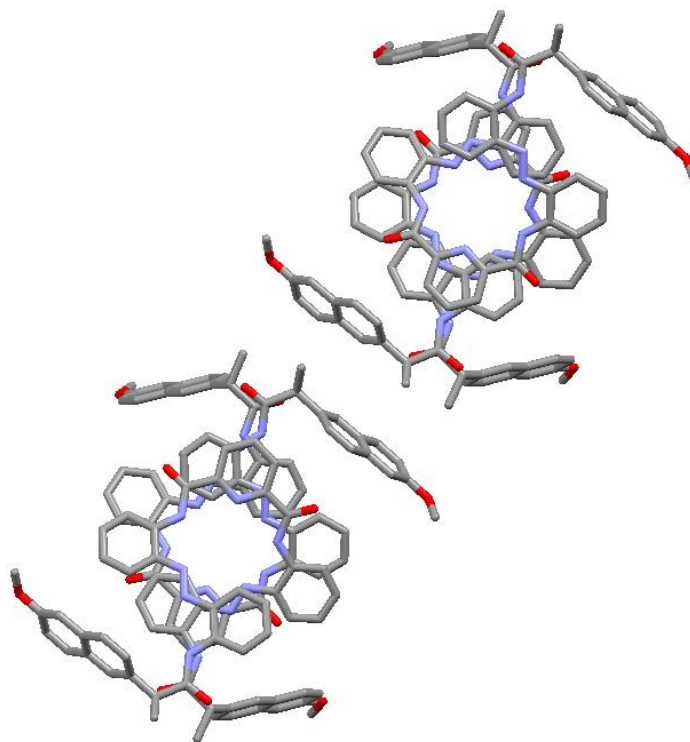


Figure S39. Solid state analysis of **1** highlighting the crystal packing of **1** showing the central cavity in the columnar stacks in the unit cell as viewed down the *a* axis. H atoms and chloroform solvent molecules have been removed for clarity.

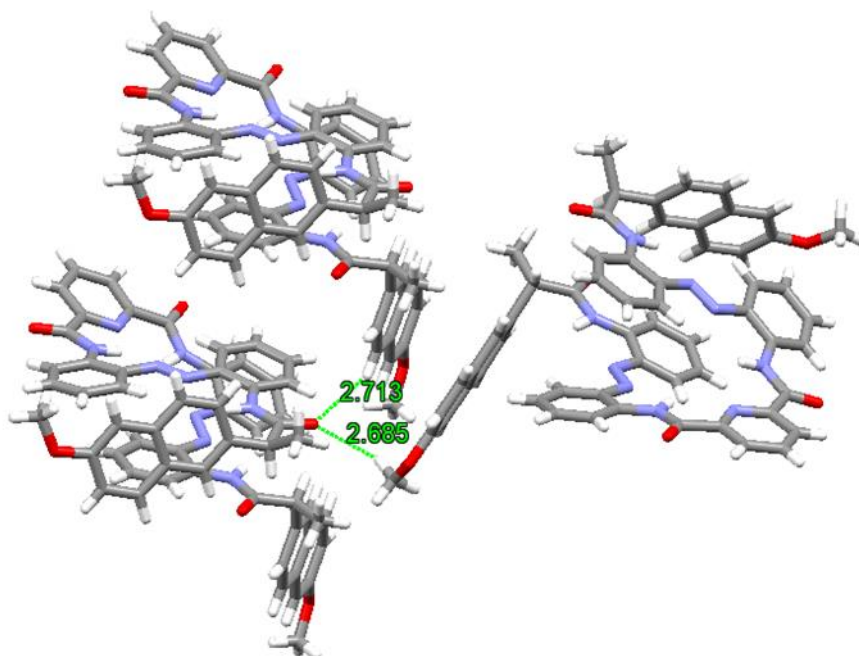


Figure S40. Solid state analysis of **1** highlighting the presence of a bifurcated intermolecular C-H...O interactions^{10,11} between three molecules. The bifurcated interaction is formed between the O atom of the carbonyl group in the amide bond of one molecule and, firstly, an aliphatic proton in the terminal ester group of an adjacent molecule and, secondly, with an aromatic proton on the naphthalene moiety of another adjacent molecule.

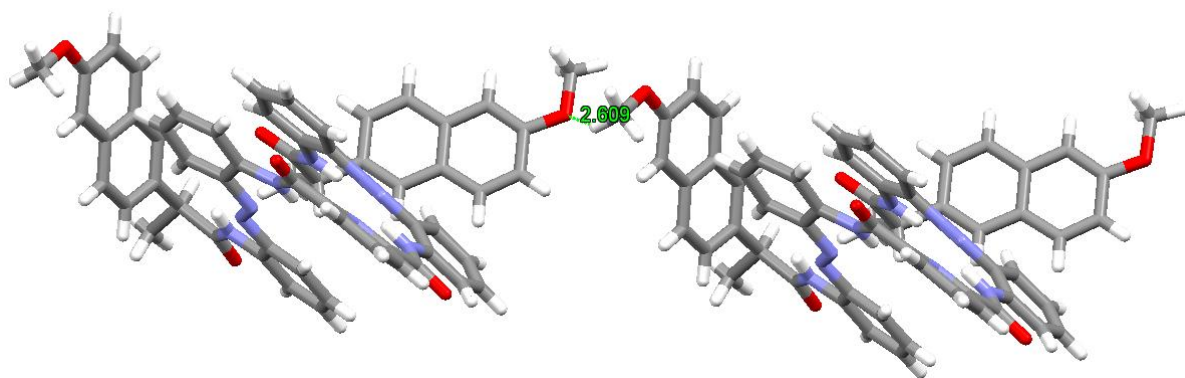


Figure S41. Solid state analysis of **1** highlighting the presence of an intermolecular C-H \cdots O hydrogen-bonding interaction^{10,11} between the O atom on the terminal ether group of one molecule and the aliphatic proton on the methyl ether group of an adjacent molecule.

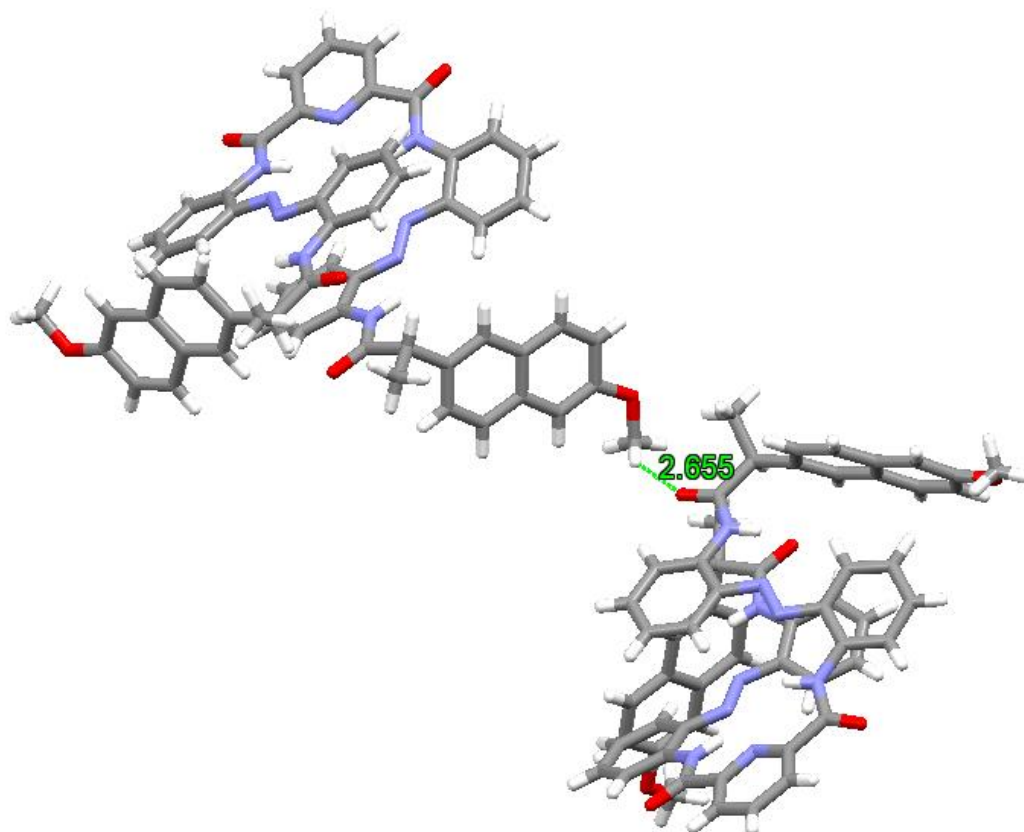


Figure S42. Solid state analysis of **1** highlighting the presence of an intermolecular C-H \cdots O hydrogen-bonding interaction^{10,11} between the O atom on the carbonyl bond of the terminal amide group and the aliphatic proton on the methyl ether group of an adjacent molecule.

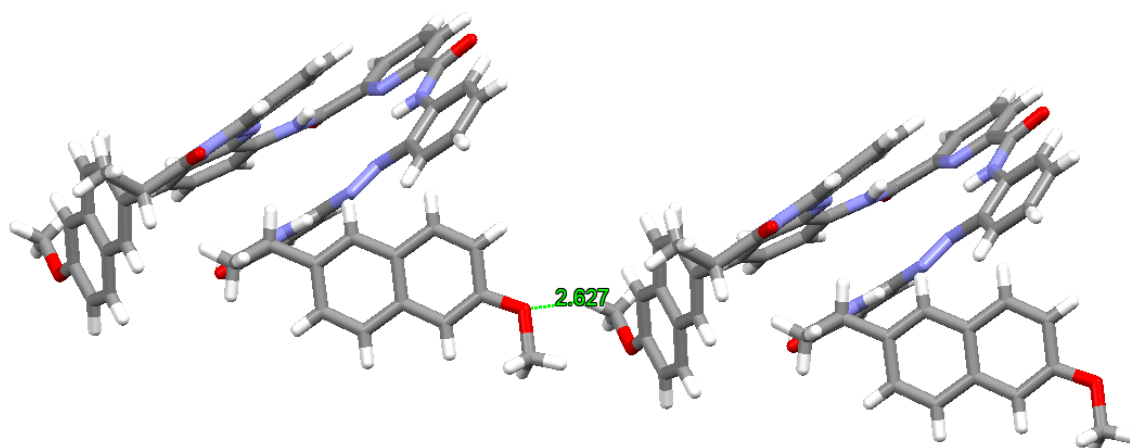


Figure S43. Solid state analysis of **1** highlighting the presence of an intermolecular C-H \cdots O hydrogen-bonding interaction^{10,11} between the O atom on the terminal ether group of one molecule and the aliphatic proton on the methyl ether group of an adjacent molecule.

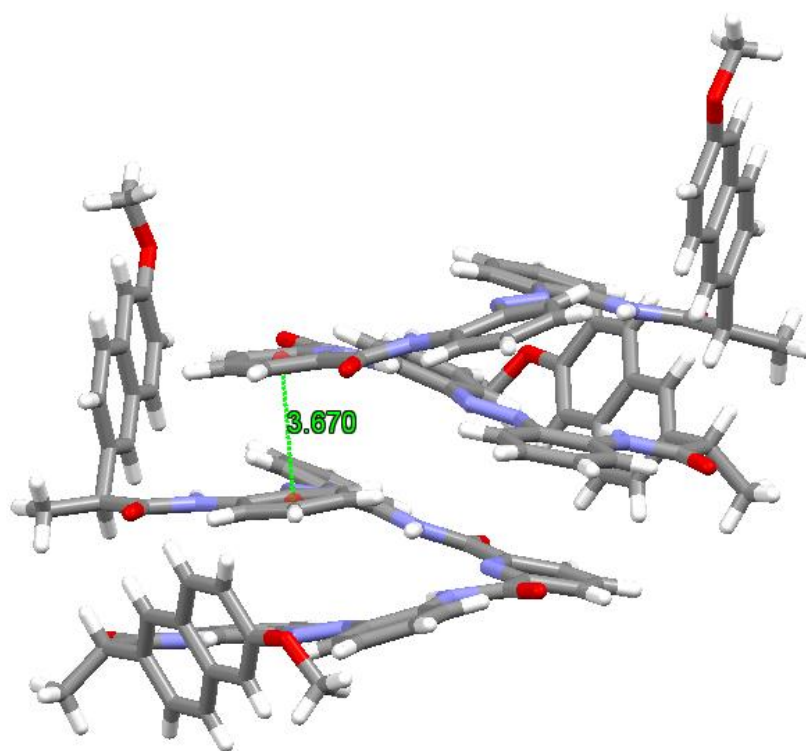


Figure S44. Solid state analysis of **1** highlighting the presence of an off-set face-to-face intermolecular π - π stacking interaction¹² between the central pyridine on one molecule and the rings on adjacent molecules.

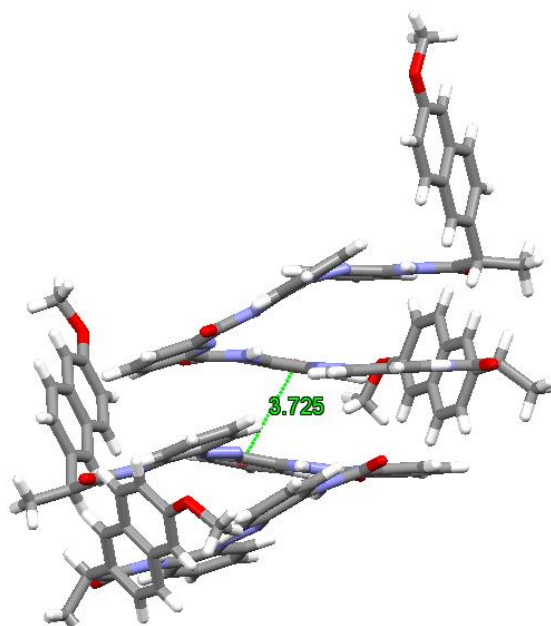


Figure S45. Solid state analysis of **1** highlighting the presence of an off-set face-to-face intermolecular π - π stacking interactions¹² between 1-azo,2-pyridinecarboxamide rings on adjacent molecules.

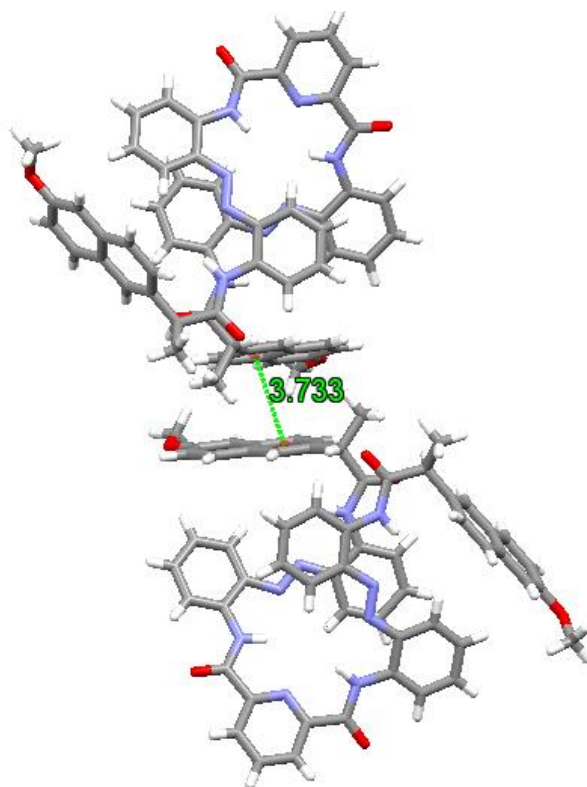


Figure S46. Solid state analysis of **1** highlighting the presence of an off-set face-to-face intermolecular π - π stacking interactions¹² between the rings in the terminal groups on adjacent molecules.

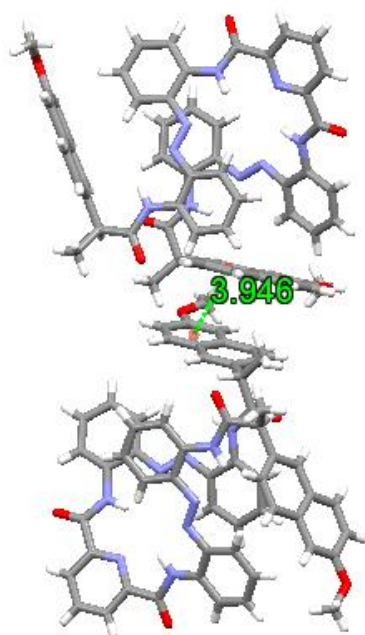


Figure S47. Solid state analysis of **1** highlighting the presence of an off-set face-to-face intermolecular π - π stacking interactions¹² between the rings in the terminal groups on adjacent molecules.

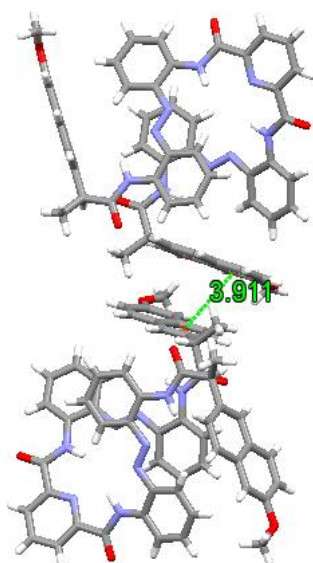


Figure S48. Solid state analysis of **1** highlighting the presence of an intermolecular off-set face-to-face π - π stacking interaction¹² between the rings in the terminal groups on adjacent molecules.

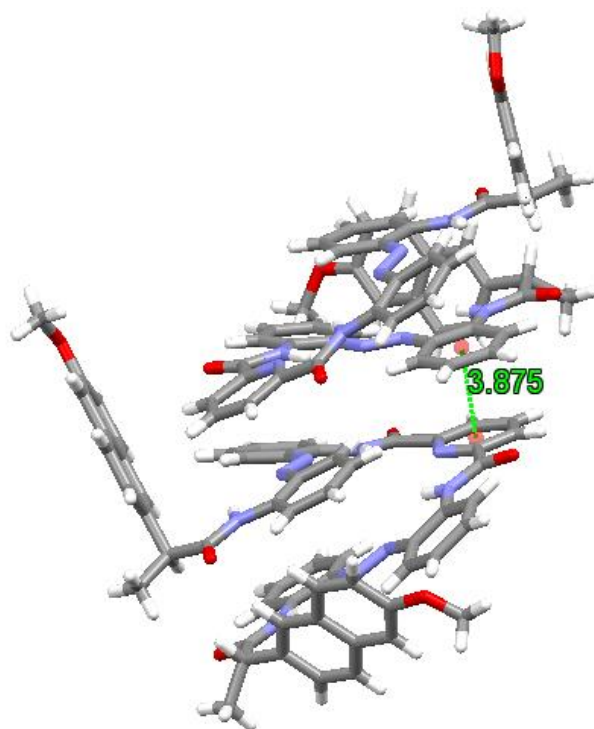


Figure S49. Solid state analysis of **1** highlighting the presence of an off-set face-to-face intermolecular π - π stacking interactions¹² between the central pyridyl ring and the 1-azo,2-amidophenyl ring on adjacent molecules.

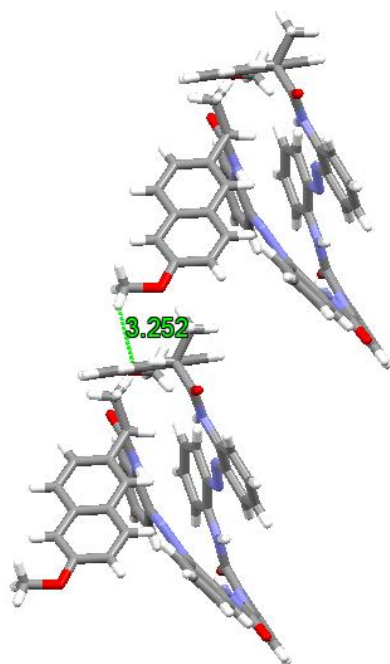


Figure S50. Solid state analysis of **1** highlighting the presence of an intermolecular C-H- π stacking interaction¹³ between an aliphatic proton on the terminal methyl ether group of one molecule and a ring in the terminal group on adjacent molecules.

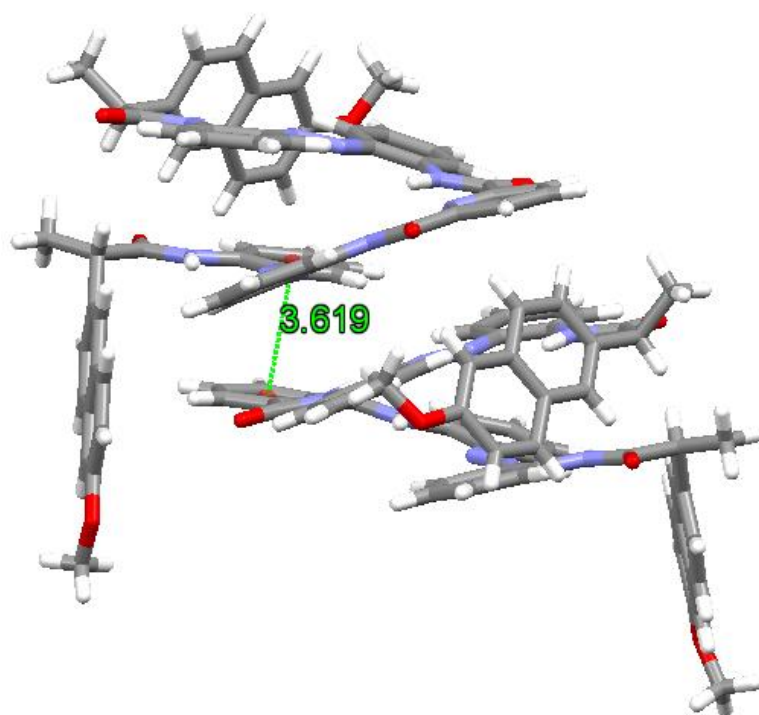


Figure S51. Solid state analysis of **1** highlighting the presence of an off-set face-to-face intermolecular π - π stacking interaction¹² between the central pyridyl ring and the 1-azo,2-amidophenyl ring on adjacent molecules.

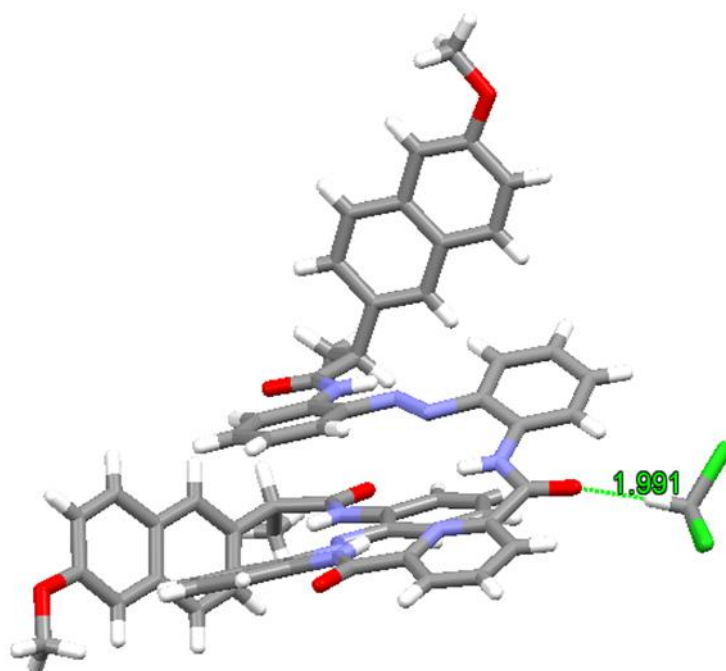


Figure S52. Solid state analysis of **1** highlighting the presence of an intermolecular $\text{Cl}_3\text{C-H}\cdots\text{O}$ hydrogen-bonding interaction¹⁴ between the H atom on a chloroform solvent molecule and the O atom of the carbonyl group of the central pyridine carboxamide moiety of **1** of an adjacent molecule.

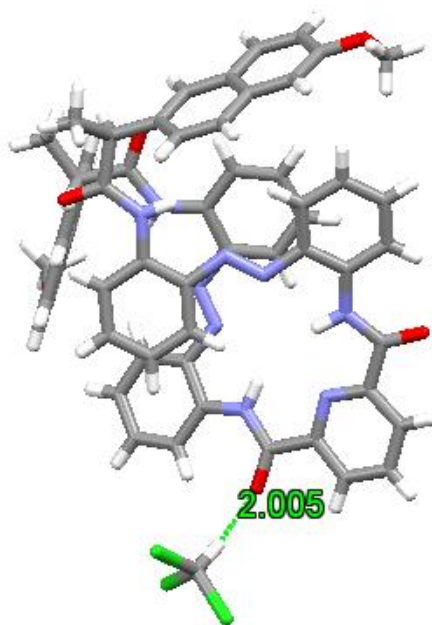


Figure S53. Solid state analysis of **1** highlighting the presence of an intermolecular $\text{Cl}_3\text{C-H}\cdots\text{O}$ hydrogen-bonding interaction¹⁴ between the H atom on a chloroform solvent molecule and the O atom of the carbonyl group of the central pyridine carboxamide moiety of **1** of an adjacent molecule.

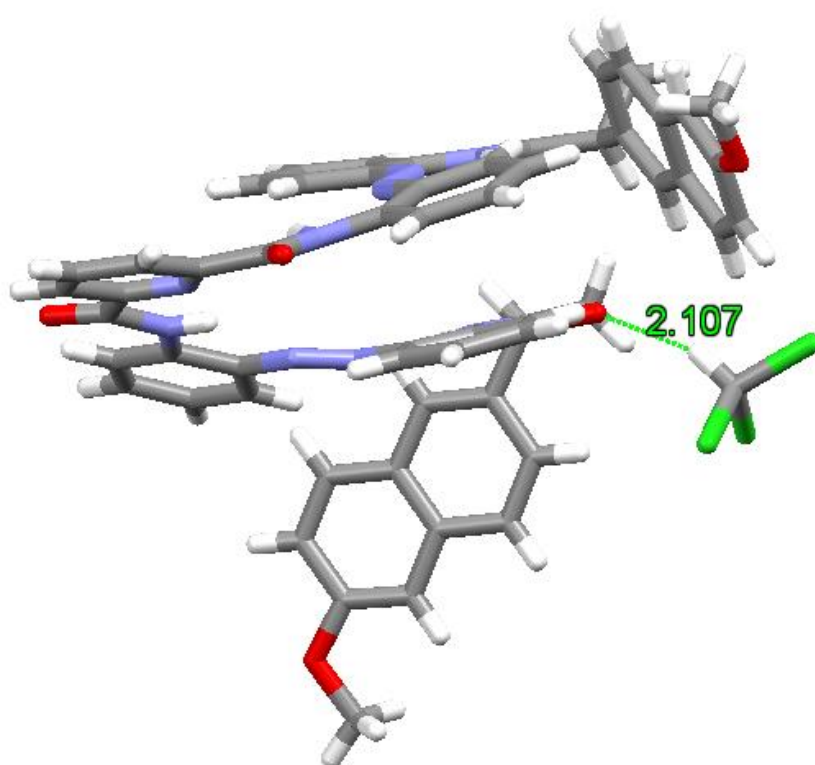
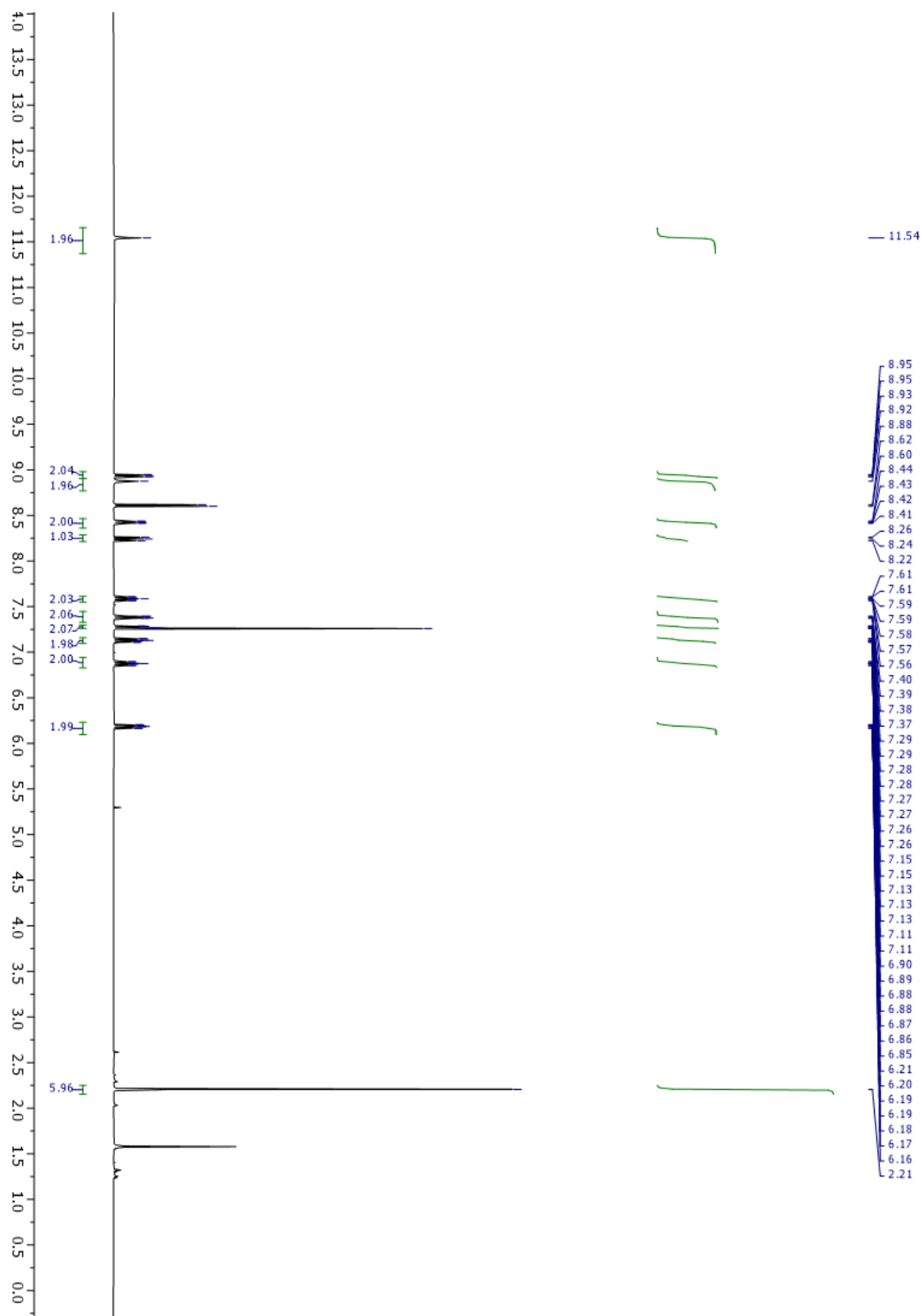
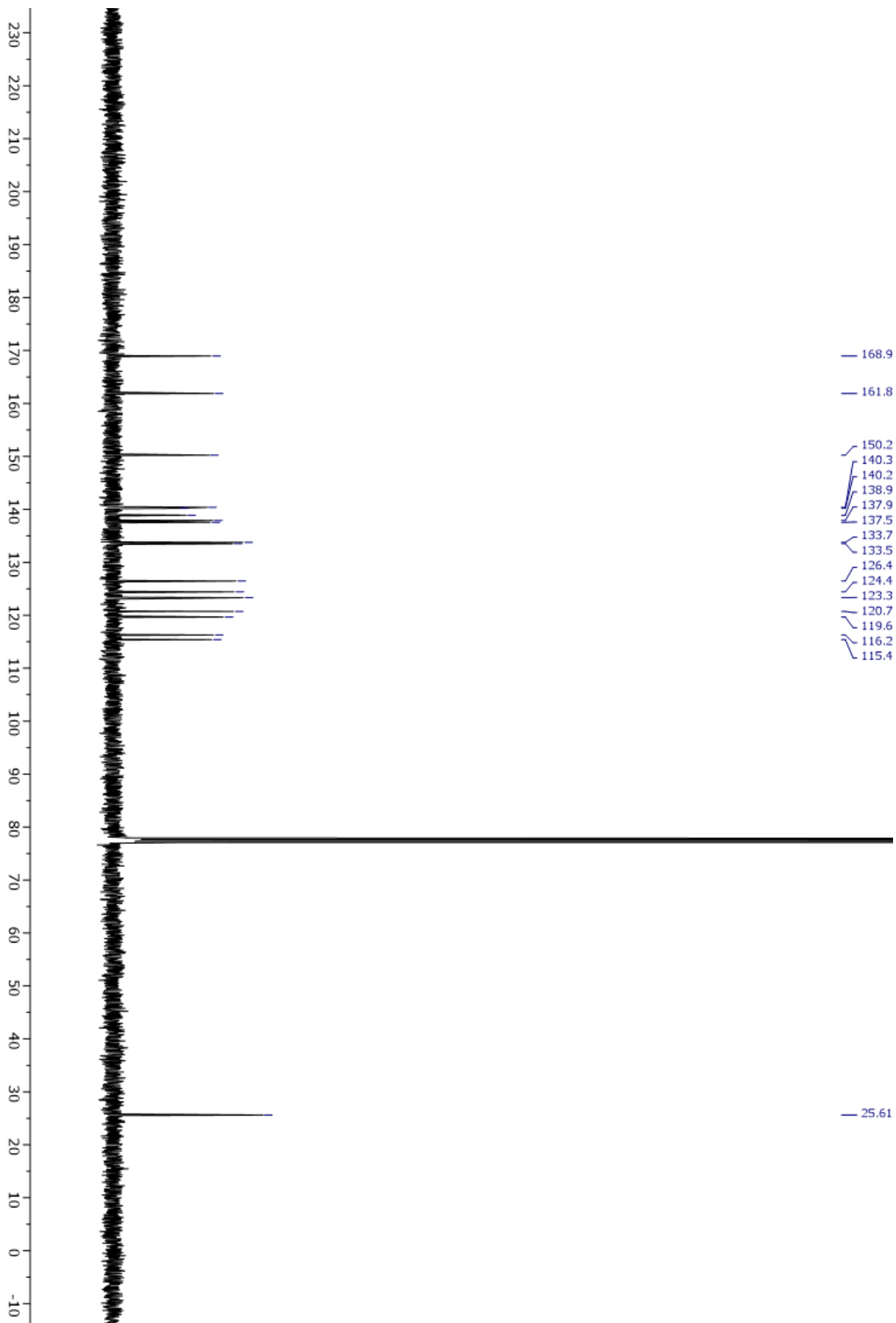


Figure S54. Solid state analysis of **1** highlighting the presence of an intermolecular $\text{Cl}_3\text{C-H}\cdots\text{O}$ hydrogen-bonding interaction¹⁴ between the H atom on a chloroform solvent molecule and the O atom of the carbonyl group of amide bond on **1** of an adjacent molecule.

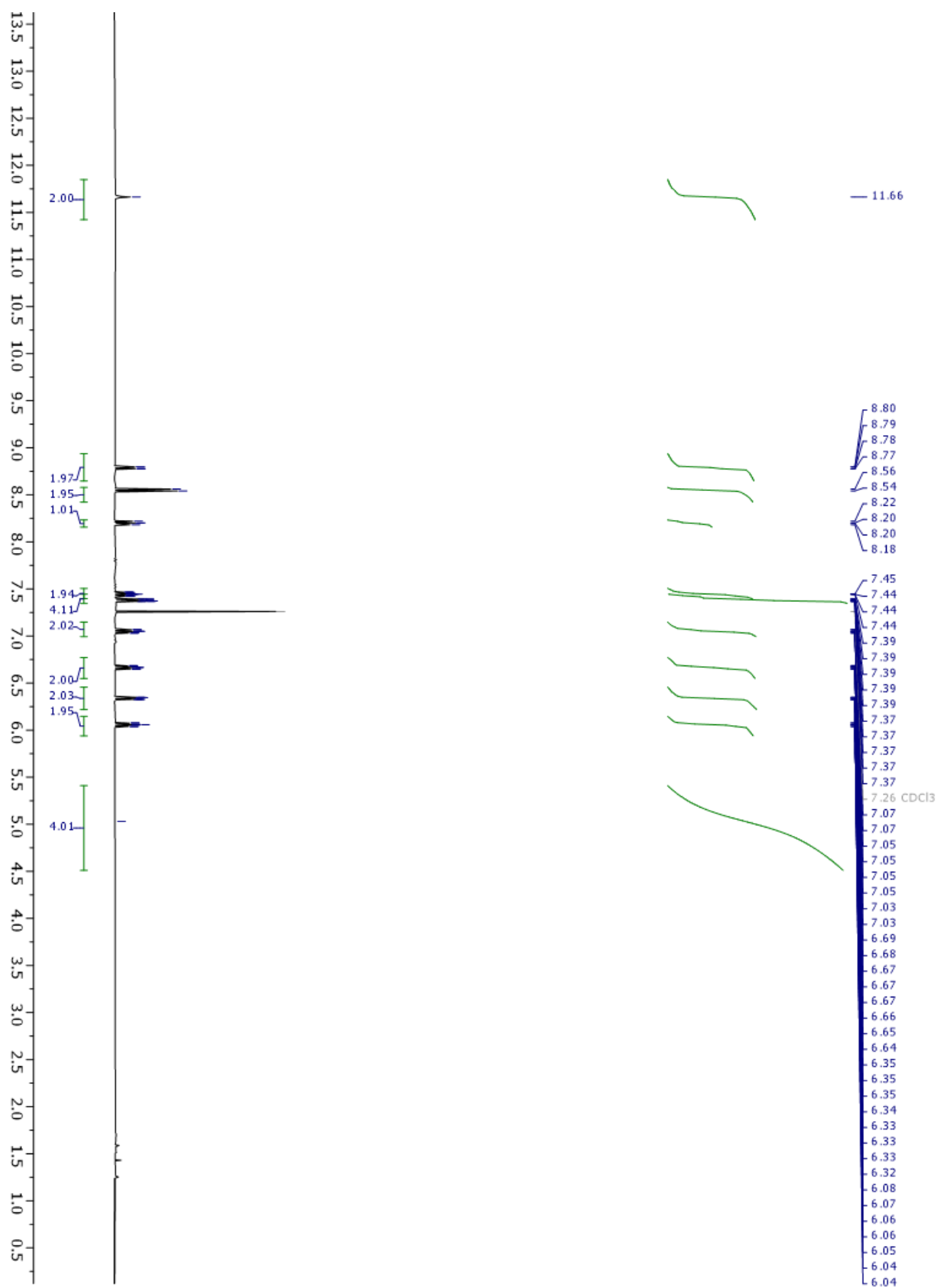
Appendix: ^1H and ^{13}C NMR spectra



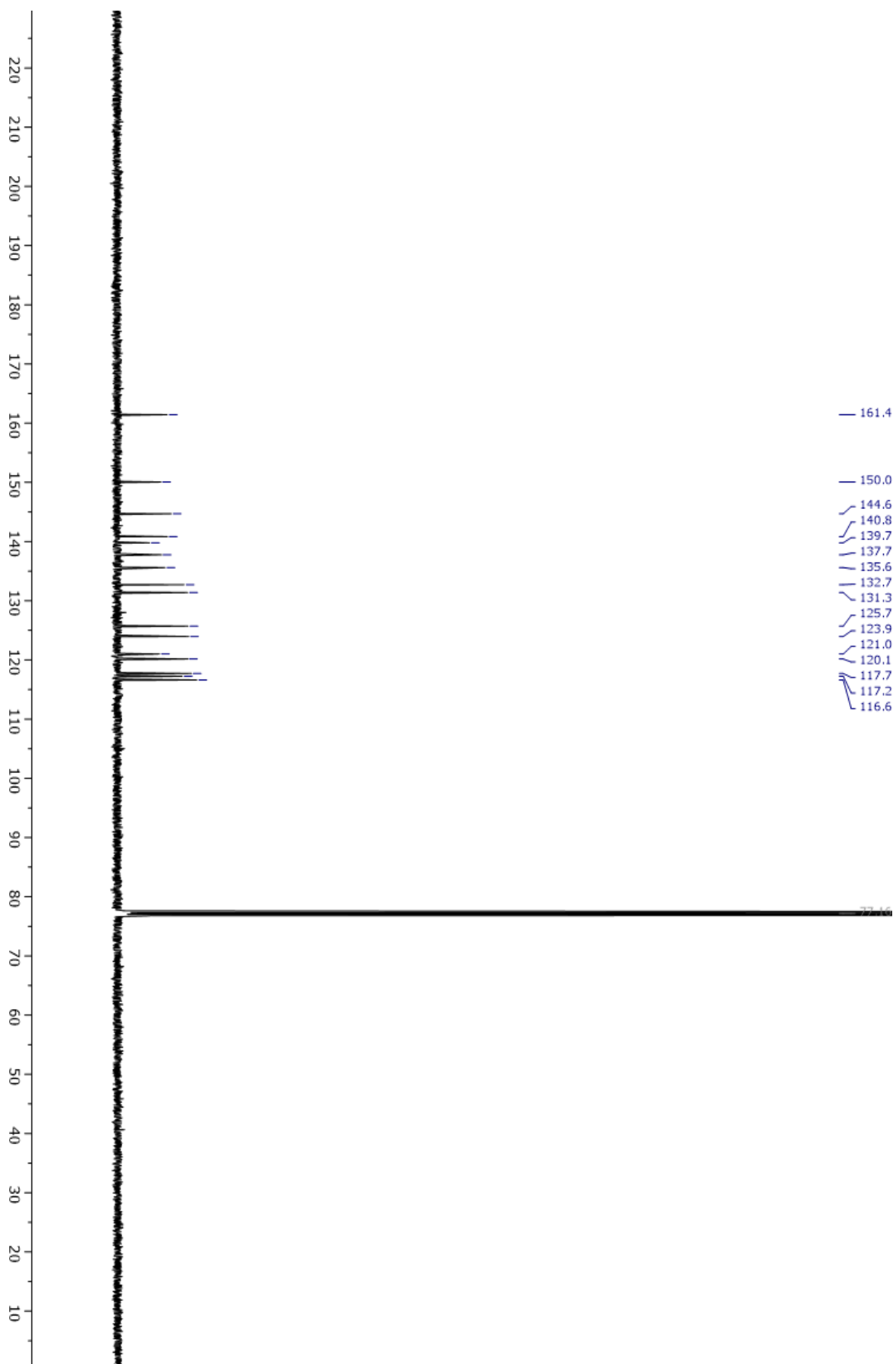
^1H NMR (400 MHz, CDCl_3 , 298 K) of 5



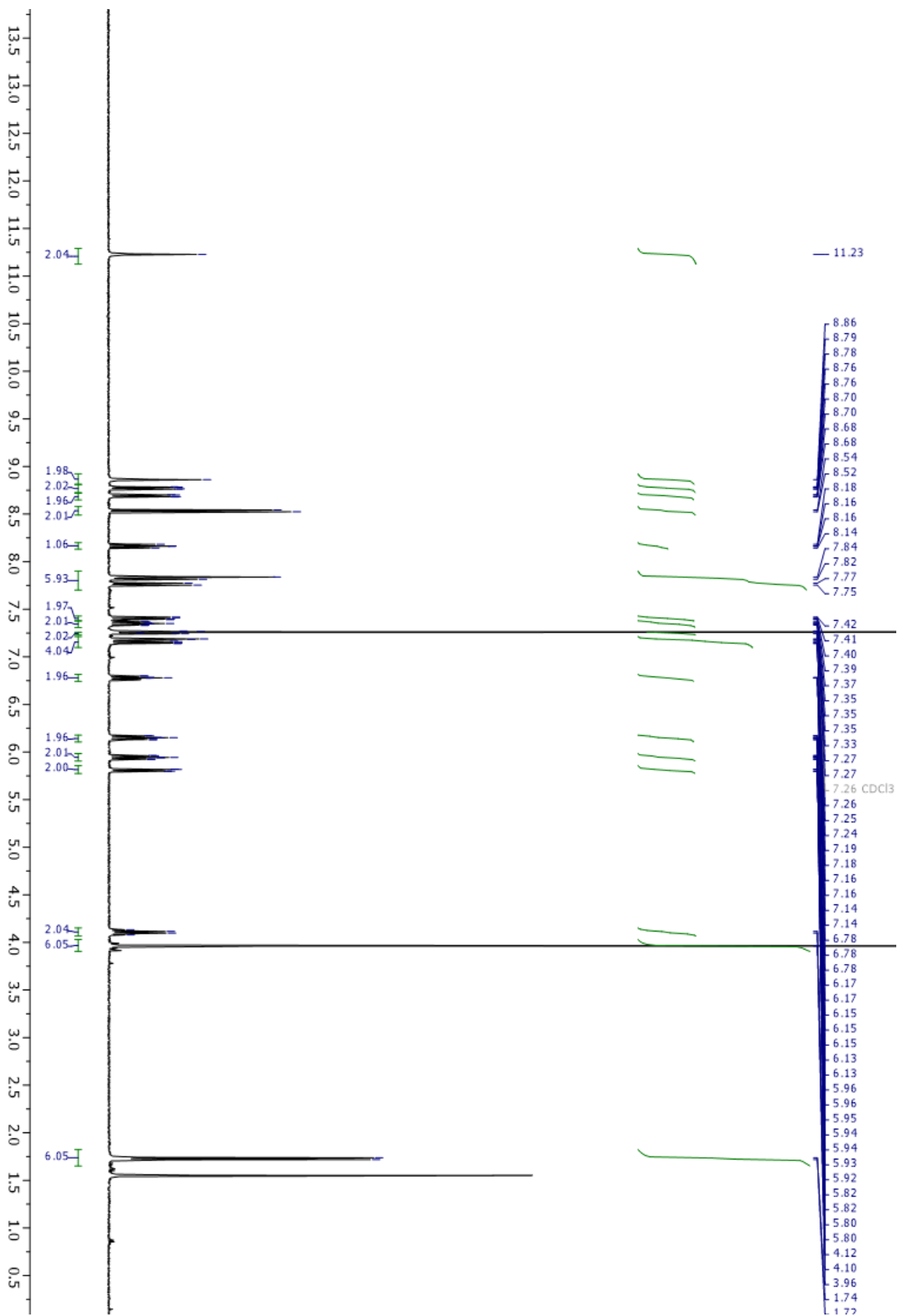
^{13}C NMR (100 MHz, CDCl_3 , 298 K) of 5



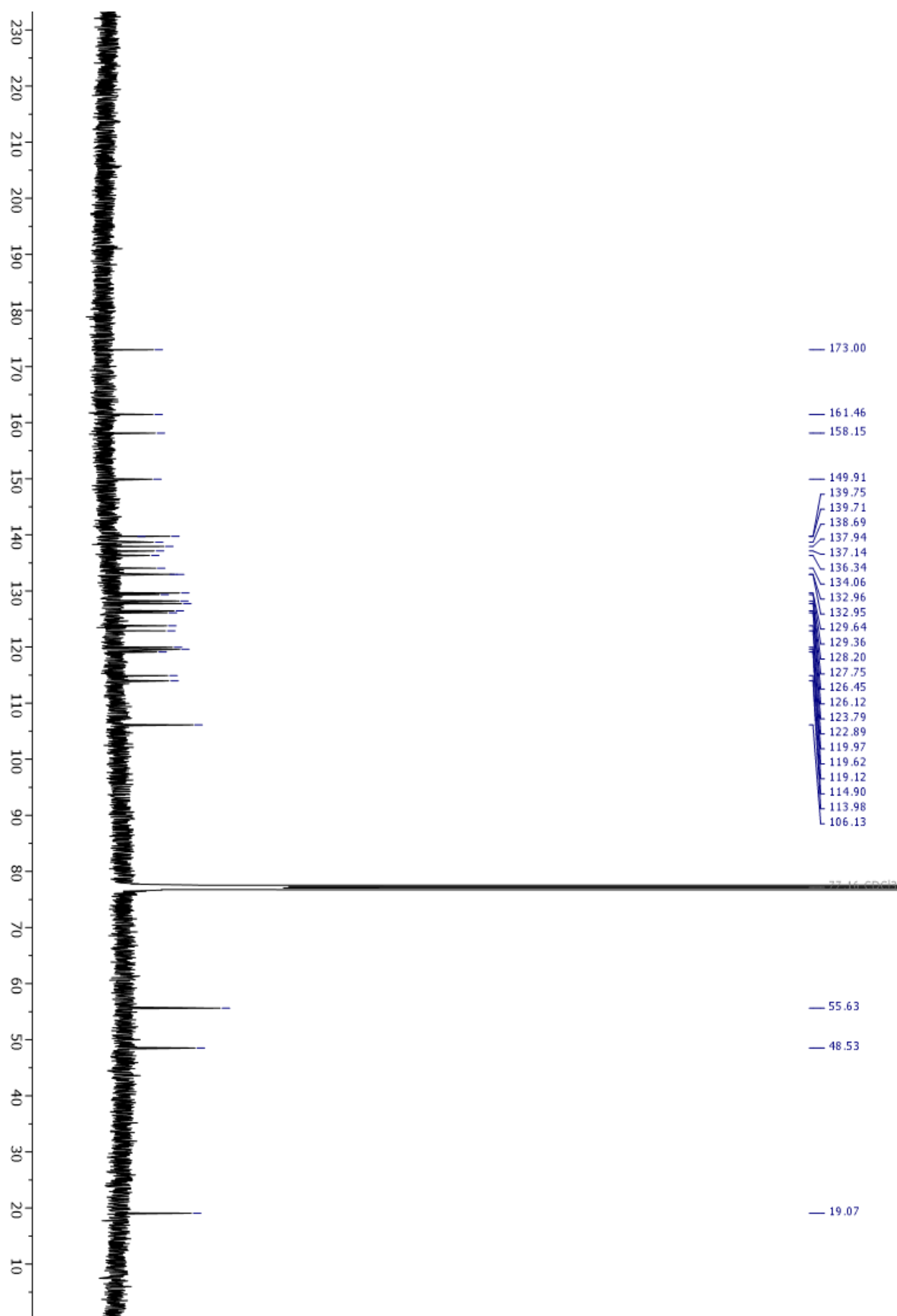
¹H NMR (400 MHz, CDCl₃, 298 K) of 6



¹³C NMR (100 MHz, CDCl₃, 298 K) of 6



¹H NMR (400 MHz, CDCl₃, 298 K) of 1



¹³C NMR (100 MHz, CDCl₃, 298 K) of 1

References

1. S. Bellotto, R. Reuter, C. Heinis, H. A. Wegner, *J. Org. Chem.*, **2011**, 76, 9826.
2. S. J. Pike, A. Heliot, C. C. Seaton, *CrystEngComm.*, **2020**, 22, 5040.
3. O. V. Dolomanov, L. J. Bourhis, R. J. Gildea, J. A. K. Howard, H. Puschmann, *J. Appl. Cryst.*, **2009**, 42, 339.
4. G. M. Sheldrick, *Acta Crystallogr. Sect. A: Found. Crystallogr.*, **2015**, A71, 3.
5. G. M. Sheldrick, *Acta Crystallogr. Sect. C: Found. Crystallogr.*, **2015**, C71, 3.
6. CrysAlisPro, Rigaku Oxford Diffraction, **2021**.
7. I. Rozas, I. Alkorta, J. Elguero, *J. Phys. Chem. A*, **1998**, 48, 9925.
8. Y. Hamuro, S. J. Geib, A. D. Hamilton, *Angew. Chem. Int. Ed.*, **1994**, 33, 446.
9. Close contacts between the amide NHs and adjacent azo nitrogens have been observed in related pyridinecarboxamide/*m*-(phenylazo)benzene oligomers see: C. Tie, J. C. Gallucci, J. R. Parquette, *J. Am. Chem. Soc.*, **2006**, 128, 1162.
10. S. Horowitz, R. C. Trievel, *J. Biol. Chem.*, **2012**, 287, 41576.
11. S. Sarkhel, G. R. Deiraju, *Proteins*, **2004**, 54, 247.
12. M. Egli, V. Tereshko, G. N. Mushudov, R. Sunushvilli, X. Liu, F. D. Lewis, *J. Am. Chem. Soc.*, **2003**, 125, 10842.
13. C. R. Martinez, B. L. Iverson, *Chem. Sci.*, **2012**, 3, 2191.
14. F. H. Allen, P. A. Wood, P. T. A. Galek, *Acta Crystallogr.*, **2013**, B69, 379.